Light-directed evolution of dynamic, multi-state, and computational protein functionalities

Vojislav Gligorovski[1], Marco Labagnara[1], Sahand Jamal Rahi[1,*]

[1]: Laboratory of the Physics of Biological Systems, Institute of Physics, EPFL, Switzerland

[*]: sahand.rahi@epfl.ch

Abstract

Directed evolution is a powerful method in biological engineering. Current approaches draw on time-invariant selection mechanisms, ideal for evolving steady-state properties such as enzymatic activity or fluorescence intensity. A fundamental problem remains how to continuously evolve dynamic, multi-state, or computational functionalities, e.g., on-off kinetics, state-specific activity, stimulus-responsiveness, or switching and logic capabilities. These require selection pressure on all of the states of a protein of interest (POI) and the transitions between them. We realized that optogenetics and cell cycle oscillations could be leveraged for a novel directed evolution paradigm ('optovolution') that is germane for this need: We designed a signaling cascade in budding yeast where optogenetic input switches the POI between off (0) and on (1) states. In turn, the POI controls a Cdk1 cyclin, which in the re-engineered cell cycle system is essential for one cell cycle stage but poisonous for another. Thus, the cyclin must oscillate (1-0-1-0…) for cell proliferation. In this system, evolution can act efficiently on the dynamics, transient states, and input-output relations of the POI in every cell cycle. Further, controlling the pacemaker, light, directs and tunes selection pressures. Optovolution is *in vivo*, continuous, self-selecting, and efficient. We first evolved two optogenetic systems, which relay 0/1 input to 0/1 output: We obtained 25 new variants of the widely used LOV transcription factor El222 that were stronger, less leaky, or green- and red-responsive. The latter was conjectured to be impossible for LOV domains but is needed for multiplexing and lowering phototoxicity. Evolving the PhyB-Pif3 optogenetic system, we discovered that loss of *YOR1* makes supplementing the expensive and unstable chromophore phycocyanobilin (PCB) unnecessary. Finally, we demonstrate the generality of the method by evolving a destabilized rtTA transcription factor, which performs an AND operation between transcriptional and doxycycline input. Optovolution makes coveted, difficult-to-change protein functionalities continuously evolvable.

Introduction

Directed evolution has been critical to improving and diversifying many of the molecular tools currently used in research and industry such as enzymes[1–5], fluorescent proteins[6,7], and antibodies[8,9]. The method relies on mutations from global or targeted mutagenesis[10–12] to diversify genetically encoded molecules. These are then screened for a desired function. The mutation-screen cycle is generally repeated to bring the molecules' functionalities closer to the desired goal.[13]

A key innovation in the field has been to couple a molecule of interest's functionality to organismal fitness obviating external intervention and screening. Such 'continuous' directed evolution methods rely on *in vivo* self-selection, which substantially simplifies and speeds up experiments, facilitating scale-up.[1,14–18] Current continuous directed evolution methods, however, use time-invariant selection mechanisms based on, for example, the strength of binding or of transcriptional activation, which are steady-state functionalities. These mechanisms can be combined to achieve complex but non-dynamic functionalities by simultaneously selecting for and against different goals[19–27] (see **Supplementary Note 1** for a partial list of previous continuous multiple-goal directed evolution experiments).

Thus, existing continuous directed evolution paradigms are poorly suited for the many natural and synthetic biological molecules that can be in different states and can dynamically switch between them. In fact, all signal transduction, control, and computation necessarily involve changes between states, usually, on (1) or off (0). For example, many transcription factors and kinases are controlled by upstream signals. In addition to relaying signals, proteins and circuits often integrate multiple inputs for cellular decisions, e.g., the amount of DNA damage and arrest times jointly determine the DNA damage checkpoint override decision.[28] Such computational capabilities are highly desirable. Building cells with more sophisticated decision-making capabilities needs logic gating, which has been created by rational design.[29–33] Evolving such proteins requires, in principle, that selection pressure is simultaneously applied on all of the computations, that is, all input-output relationships of the POI. Otherwise, if directed evolution is performed for only one state, the other states or the ability to switch to them can be corrupted.[34] For example, long-term directed evolution of GPCRs under constant ligand concentrations reduces ligand responsiveness.[35]

To address this need, researchers have developed non-continuous directed evolution methods, in which time-invariant selection mechanisms are alternated to screen each POI state sequentially[36–70] (see **Supplementary Note 2** for a partial list of past alternating selection/counterselection experiments). In these methods, two steps are typically repeated: an assay for on (1) activity is performed under inducing conditions, then an assay for off (0) activity under non-inducing conditions. In practice, selection and counterselection are performed with alternating media

conditions, e.g., -uracil and +5-fluoroorotic acid[71], or changing fluorescence-activated cell sorting (FACS) gates. While creative, these approaches require interventions involving labor or specialized instrumentation or both. Furthermore, one cycle of selection and counterselection based on media switches and cell proliferation took 8-64 hrs with bacteria or 2-5 days with yeast. This timescale determines the selection pressure placed specifically on the kinetics of the POI switch cycle, which is typically desired to be much shorter.

The ability to perform directed evolution that is both continuous and germane for dynamic, multi-state, and computational protein functionalities would advance biological engineering. Here, we present the first such paradigm, which we name 'optovolution'. In contrast to previous approaches, optovolution was designed with a mechanism to evolve all input-output relationships of a POI as well as switches among them continuously. Two conceptual advances, explained in more detail below, underlie optovolution: By engineering a POI to control a cell cycle regulator that is essential for one step of cell proliferation but toxic to another, the POI must evolve or maintain the ability to switch between 0 and 1 outputs rapidly, twice in each cell cycle. The selection mechanism is inherently dynamic. Secondly, by controlling the input to the POI with light and optogenetics, the selection pressure is shaped by an external signal that is also dynamic at the timescale of a cell cycle.

We apply optovolution to three systems, the optogenetic transcriptional system El222 and the optogenetic protein-protein interaction system PhyB-Pif3, which relay light input by switching on (1) or off (0), and an AND gate, in which a degron-tagged rtTA transcription factor is controlled by transcription and doxycycline. The dynamic, multi-state properties of these proteins make them unsuitable for existing continuous directed evolution paradigms:

1) LOV domains make up the core of most non-ion-channel optogenetic systems[72–80,80–86], presumably because they are small, reliable, and do not need exogenous chromophores. Interest in LOV domains has spurred past diversification work[54,87–89]. The LOV transcription factor El222, in particular, is widely used in many biological models from cell-free systems[90], to bacteria[91], yeast[92,93], mammalian cell lines[94,95], and zebrafish[96]. (See **Supplementary Note 3** for additional information regarding El222.) In comparison to other inducible transcriptional systems, El222 controlling the standard *light-inducible promoter* (*LIP*) has both more off-state leakiness and lower on-state strength than, for example, the *GAL1* promoter, demonstrating potential room for improvement.[88] Less leaky or more light-sensitive variants are desirable for different applications: Low leakiness is necessary when controlling toxic genes such as endonucleases; higher output under less light allows reducing phototoxicity.[88] Further, all existing LOV systems are only activated by blue light, which has several drawbacks: First, blue light is more phototoxic than longer-wavelength light.[88,97] Secondly, blue light penetrates skin poorly.[98] Thirdly, the advantages of LOV domains cannot be leveraged to control different optogenetic systems independently in an organism. Ideally, one could build optogenetic systems based on LOV domains, change their color responsiveness by mutation, and thus straightforwardly combine different systems. Instead, for

105 multiplexing with LOV domains, other light-sensitive domains have to be used as well, each
106 representing a challenging endeavor to combine with other proteins.[99–102] In fact, substantially
107 changing the color responsiveness of LOV domains was conjectured to be "likely impossible"
108 based on the lack of such known natural or engineered examples and physicochemical
109 considerations.[103] Previous work to shift the absorption spectrum of LOV domains with targeted
110 mutations achieved a maximal shift of 8 nm further toward UV in the absorption peak *in vitro*[104].
111 Shifts in the emission spectrum for use as fluorescent proteins have also been attained.[105] Using
112 optovolution, we evolved 25 new variants of El222, including more light sensitive, less leaky, or
113 green- and red-responsive mutants, paving the way for new applications.

114 2) In the widely used PhyB-Pif3 system, PhyB and Pif3 dimerize in response to red light and
115 dissociate with far red light. The system is often used to change the intracellular localization of
116 proteins by fusing them to PhyB or Pif3 and anchoring the other dimerization partner to a specific
117 intracellular compartment[106,107]. (See **Supplementary Note 4** for additional information regarding
118 the PhyB-Pif3 system.) For transcriptional induction, PhyB and Pif3 are fused to the Gal4
119 transcriptional activation domain (AD) and the Gal4 DNA binding domain (DBD), respectively.[108–110]
120 For use in yeast, *Caenorhabditis elegans*, and mammalian cells, the chromophore PCB has to be
121 supplemented.[106,108,111] The co-factor is expensive as well as light- and temperature-sensitive,
122 complicating experiments. In previous work, a biochemical pathway to convert heme to PCB was
123 introduced in different organisms.[111–114] This involved substantial genetic manipulation of the host
124 genome: Several transgenes had to be introduced, some of which needed to be targeted to
125 mitochondria, their expression levels needed to be optimized, and, in certain cases, endogenous
126 genes needed to be deleted. It is unclear whether there are pathways in cells that could be
127 modified for PhyB-Pif3 to work without supplemental PCB. Using optovolution, we found that loss
128 of function of *YOR1* makes PCB unnecessary in budding yeast. The use of *yor1Δ* substantially
129 simplifies applications and further directed evolution experiments.

130 3) While optovolution leverages light for directing evolution, we demonstrate the more
131 general applicability of optovolution by evolving a non-optogenetic logic gate POI. It is often
132 desirable to condition the activity of molecules on two inputs. This requires AND logic, which is
133 relatively difficult to create in biological systems. To construct such a system, we used the
134 doxycyclin-controlled transcription factor rtTA[115] and fused it to a PEST degron[116]. (See
135 **Supplementary Note 5** for additional information regarding rtTA.) This double-lock control
136 represents an AND gate function between transcriptional and doxycycline input. Without the
137 degron, rtTA protein would be stable and thus, after translation, only controlled by doxycycline;
138 responsiveness to further transcriptional input could only happen in proliferating cells at the
139 relatively slow timescale of dilution. However, the PEST-rtTA fusion protein initially produced very
140 weak output. With optovolution, we evolved two mutants that conferred substantial output from
141 the *tetO* promoter while maintaining minimal leakiness.

Optovolution is the first continuous directed evolution paradigm for dynamic, multi-state, and computational functionalities. We demonstrate its usefulness by uncovering unexpected and useful mutations improving three different important molecular tools.

Results

Conceptual requirements for evolving dynamic, multi-state, and computational properties

We started with a general theoretical analysis. We considered how to evolve a POI with one or more inputs and one output, each of which can be in the 0 or 1 state (Fig. 1 A). The POI needs to fulfill the basic requirement for computational capability: each of the two output states can be produced by certain inputs, at least, by the end of directed evolution. This exclude the possibility of evolving proteins that switch purely stochastically between states, without input, or whose inputs and outputs are practically inaccessible (**Discussion**).

As in electrical engineering, 0 and 1 are useful abstractions, which here represent molecular activity. Characterizing a POI in terms of input-output relationships simplifies the description of a wide range of directed evolution goals. These may include increasing, lowering, or changing the nature of the activity of outputs for specific inputs, or modifying the kinetics of switching between outputs. 0 or 1 need not refer to absolute zero or the maximally attainable activity. We considered that there can be a single input i to the POI, for example, transcriptional induction of the POI, or a complex input $\boldsymbol{i}=(i_1,\ldots,i_n)$ such as specific phosphorylation patterns at n residues of the POI.

For such a set of possible inputs and outputs, the main conceptual challenge was to find a mechanism to perform selection on each input-output relationship of the POI and the kinetics of the transitions. We suppose that the inputs are labeled $\boldsymbol{i_a}$, $\boldsymbol{i_b}$, $\boldsymbol{i_c}$, $\boldsymbol{i_d}$, … and correspond to desired POI outputs 1, 0, 1, 0, … We realized that we could perform continuous directed evolution on this system if we made the POI fully control a cellular regulator that was essential for one step in cell proliferation but poisonous for another (Fig. 1 B, C). In such a system, if the POI switches between 1-0-1-0-… outputs, driven by repeated cycles of inputs $\boldsymbol{i_a}$-$\boldsymbol{i_b}$-$\boldsymbol{i_c}$-$\boldsymbol{i_d}$-…, then cells will proliferate maximally (Fig. 1 D). Any error, either in switching speed or state, e.g., POI output sequence 1-1-1-0-…, causes skipped cell cycles, incurring a substantial fitness penalty and giving an advantage to mutants with better fidelity to the desired input-output relationships. There is freedom in devising protocols for the $\boldsymbol{i_a}$-$\boldsymbol{i_b}$-$\boldsymbol{i_c}$-$\boldsymbol{i_d}$-… inputs. How to sequence the inputs optimally represents an interesting mathematical problem, which we solved for time-independent protocols in **Supplementary Mathematical Analysis**.

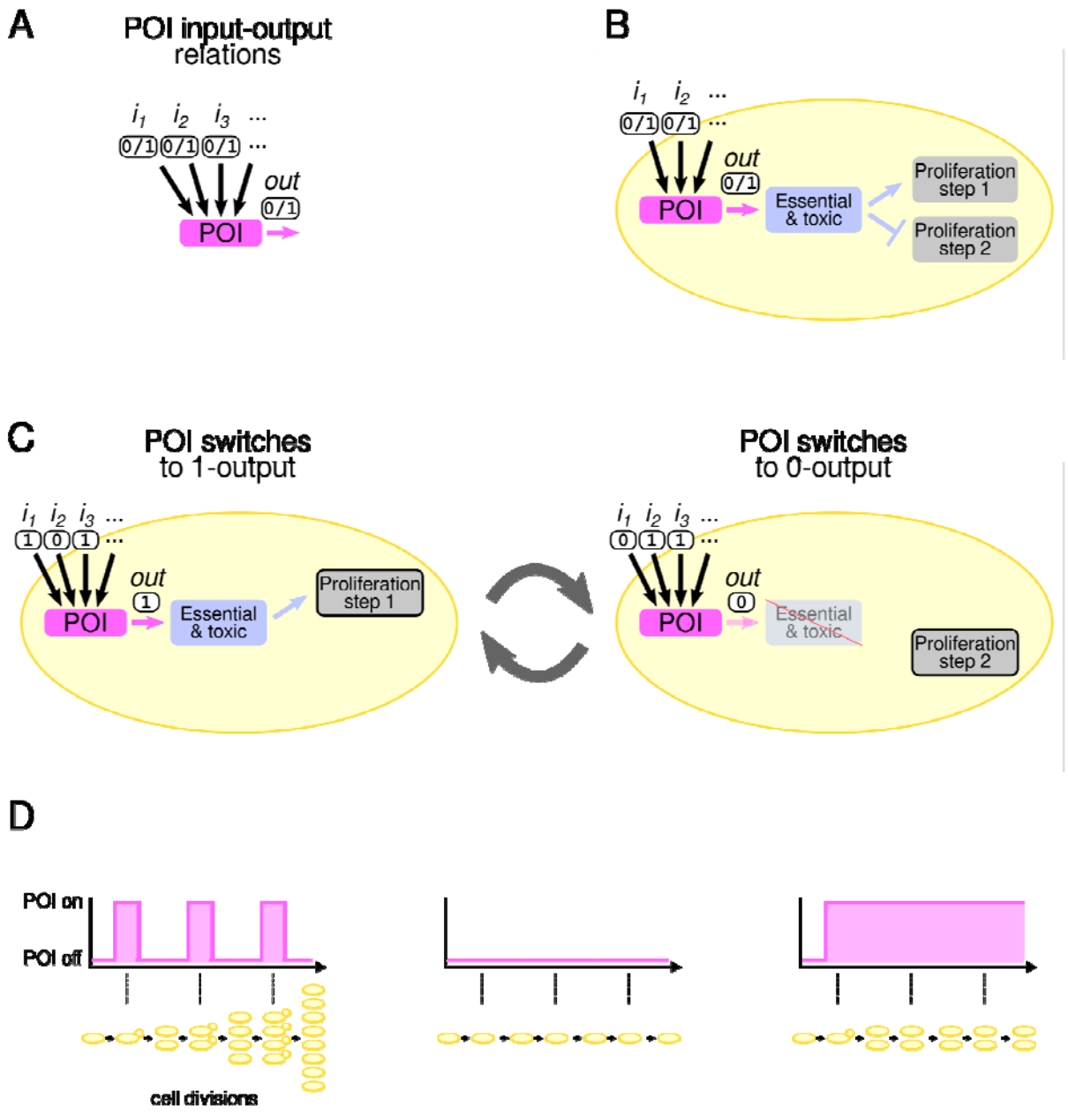

Figure 1. Conceptualization of optovolution. A: The POI has one or multiple inputs and one output. Inputs and output are idealized as having two states, on (1) or off (0). B. In optovolution, the POI controls a cellular regulator that is essential for one step in cellular proliferation but poisonous for another. The inputs to the POI are most conveniently controlled by light, mediated by optogenetic systems, which are not shown. C. By cycling the inputs to the POI, the POI switches output states and drives cycles of cellular proliferation. D. Cells only proliferate with repeated 1-0-1-0-... output pulses of the POI, not continuously on (1) or off (0) output, in a mutationally robust manner.

Practical requirements on the input and output of the POI

The inputs to the POI must be exogenously controllable. Optogenetic control of the POI inputs is compatible with continuous directed evolution since administering light, even for weeks, is

185 precise, fast, easily tunable, cheap, straightforward, and scalable. For control of non-optogenetic
186 POIs, light input can in principle be indirectly mediated through the rapidly expanding
187 optogenetics toolkit, which includes light-sensitive transcription factors, localization signals,
188 degrons, and kinases, acting on the POI.[117–122] Chemical-controlled POIs can in some instances be
189 converted to light control by swapping the relevant domains[121,123–126]. Light control has also been
190 built into POIs specifically to be used for screening for improved protein functionality.[37]
191 Nevertheless, the power of optogenetics for directing evolution has hitherto generally not been
192 recognized. While we focus on optogenetic control of the inputs to leverage the advantages of
193 continuous directed evolution, the cell cycle-coupled selection mechanism at the heart of our
194 method is in principle also compatible with chemically controlled POI inputs (**Discussion**).

195 Another requirement of our theoretical considerations is that the POI produces an output that
196 controls a regulator of cell proliferation. In principle, this control can occur in different ways but
197 we will demonstrate optovolution with systems whose output is ultimately coupled to the
198 transcription of the regulator (**Discussion**).

199 Requirements on the selection mechanism

200 To implement the above considerations, it was critical to make cell proliferation fully dependent
201 on the POI's 1-0-1-0-… output. The key idea was to find a regulator of cell proliferation, which
202 would be required for one step in proliferation but block another (Fig. 1 B-D). By engineering the
203 POI to fully control this regulator, the POI would drive one cell cycle for each 1-0 output oscillation
204 of the POI.

205 The overall system needed to satisfy stringent requirements:

206 1. Tight coupling: Each proliferation step must be tightly dependent on the switching of the
207 POI. Mutations that turn the POI constantly on (1) or off (0) should block cell proliferation (Fig. 1
208 D).

209 2. Mutational robustness: No (known) mutations should break the tight coupling of the POI
210 and cell proliferation. Such mutations would otherwise allow bypassing the selection pressure.

211 3. Reliability: A brief period of the POI's 1 output should trigger one step in cell proliferation
212 in most cells, and switching to 0 should allow the completion of the rest of a proliferative cycle.
213 Repetitive 1-0 switches at the right times should drive cells through consecutive growth-division
214 cycles.

215 4. Tolerance to poor initial performance: POIs may work too poorly to drive the system
216 initially. Genetic constructs, which we call 'training wheel plasmids', should support cell
217 proliferation initially and should be cleanly removable early in the directed evolution campaign.

218 5. Usability: Any POI with the same type of output, e.g., transcription, should be easily
219 insertable and evolvable in the same strains for directed evolution.

220 6. Stability: Over long periods of directed evolution, cells should maintain a stable genome
221 and not polyploidize, which makes genetic analyses difficult.

222 Implementation in budding yeast

223 We engineered the system in budding yeast because it has a relatively fast cell cycle (≈ 90 min
224 period in glucose medium), which has been researched extensively. A short generation time is
225 important since it sets the maximum speed with which selection pressure can be exerted on POI
226 state switching.

227 In search of a gene that is essential for one proliferative step but poisonous for another, one might
228 consider cell cycle control regulators that oscillate once per cell cycle. However, it is not obvious
229 which to choose since the cell cycle control system is remarkably robust. For example, constitutive
230 expression of *CLN2* and *CLB2* in the absence of all other Cdk1 cyclins (*cln1-3Δ clb1-6Δ*) suffices for
231 cell cycles[127]. Even in such a highly stripped-down cell cycle control system, the remaining two
232 Cdk1 cyclins do not need to oscillate transcriptionally.

233 However, past experiments showing that constant transcriptional induction suffices for cell
234 proliferation were often performed with relatively weak promoters such as *GALL*[88]. Thus, we
235 pursued a strategy in which we re-examined elements of cell cycle control for being essential for
236 one part of the cell cycle but poisonous for another, at least, when over-expressed. Once found,
237 we could engineer cells to be even more sensitive to both the need for the cell cycle regulator at
238 one cell cycle stage and poisonous for the other.

239 For our search, we used the relatively strong blue-light-induced LOV transcription factor El222 and
240 the El222-controlled *LIP* (**Supplementary Note 3**). This system allowed us to test rapid switches in
241 glucose medium, where proliferation is relatively fast. We transformed yeast with constructs, in
242 which *LIP* controlled the transcription of cell cycle regulators we wished to test (Table 1, column
243 1). In these cells, we had deleted endogenous cell cycle control genes whose absence makes the
244 corresponding inducible cell cycle gene essential. Further, cells were kept viable before our tests
245 by inducible transcriptional constructs that could be shut off for the test (Table 1, column 2). For
246 more details on cell cycle regulation in budding yeast generally and in our final strain, see
247 **Supplementary Note 6**.

Candidate cell cycle regulator controlled by El222/*LIP*	Genetic background for tests	Result
CLB2	*clb1,2Δ* *GALL-CLB2*	Constitutive overexpression failed to arrest cell cycle
CLB2kd	*clb1-6Δ swe1Δ* *GALL-CLB2*	Pulsatile expression regime could not be found for continuous cell cycles
CDC20	*cdc20Δ, cdh1Δ* *MET3pr-CDC20*	Constitutive overexpression failed to arrest cell cycle

CLN2	*cln1-3Δ* *MET3pr-CLN2*	Constitutive overexpression failed to arrest cell cycle
CLB5	*cln1-3Δ* *MET3pr-CLN2*	Oscillatory induction needed for cell cycles
CLB5	*cln1-3Δ clb3,4,6Δ* *MET3pr-CLN2*	Oscillatory induction needed for cell cycles

Table 1: Tests to identify cell cycle regulators which are needed for one part of the cell cycle but toxic for another in specially engineered genetic backgrounds. During the tests, we turned off the chemical-responsive promoters *MET3pr* and *GALL*.

We tested for three different properties: inviability given continuous off (0) or on (1) expression as well as proliferation under periodic expression. We started with the key components of the core cyclin-Cdk/APC negative feedback loop of the cell cycle (Table 1, Fig. 2 A). First, we tested optogenetic control of *CLB2*, the major M cyclin in budding yeast[128], in a *clb1,2Δ* background. As expected, in darkness, the lack of *CLB1* and *CLB2* caused cells to arrest before mitosis. However, continuous expression of *LIP-CLB2* did not prevent cells from cycling in glucose medium. Since Clb2 activity has to be reduced for cell cycle exit, we next tested whether Clb2kd, an undegradable variant of Clb2 was more suitable. Clb2kd continued to be needed for entry into mitosis and anaphase in a *clb1,2Δ* background. However, we could not find a regime of pulsing light under which cells performed continuous cell cycles. After a few cell cycles, Clb2kd blocked mitotic exit nearly permanently presumably because Sic1 inhibition and dilution did not reduce Clb2kd activity sufficiently. In previous work, budding yeast cells had been shown to be very sensitive to the duration and period of joint Start cyclin and *GAL1pr-CLB2kd* pulsing over only a few cell cycles, which was interpreted as a signature of an artificial incoherent feedback loop which had been incorporated into cell cycle control[129]. Next, testing the B-type cyclin inhibitor *CDC20*, whose deletion leads to metaphase arrest, we found that it was similarly not suitable since *LIP-CDC20* overexpression did not arrest cells.

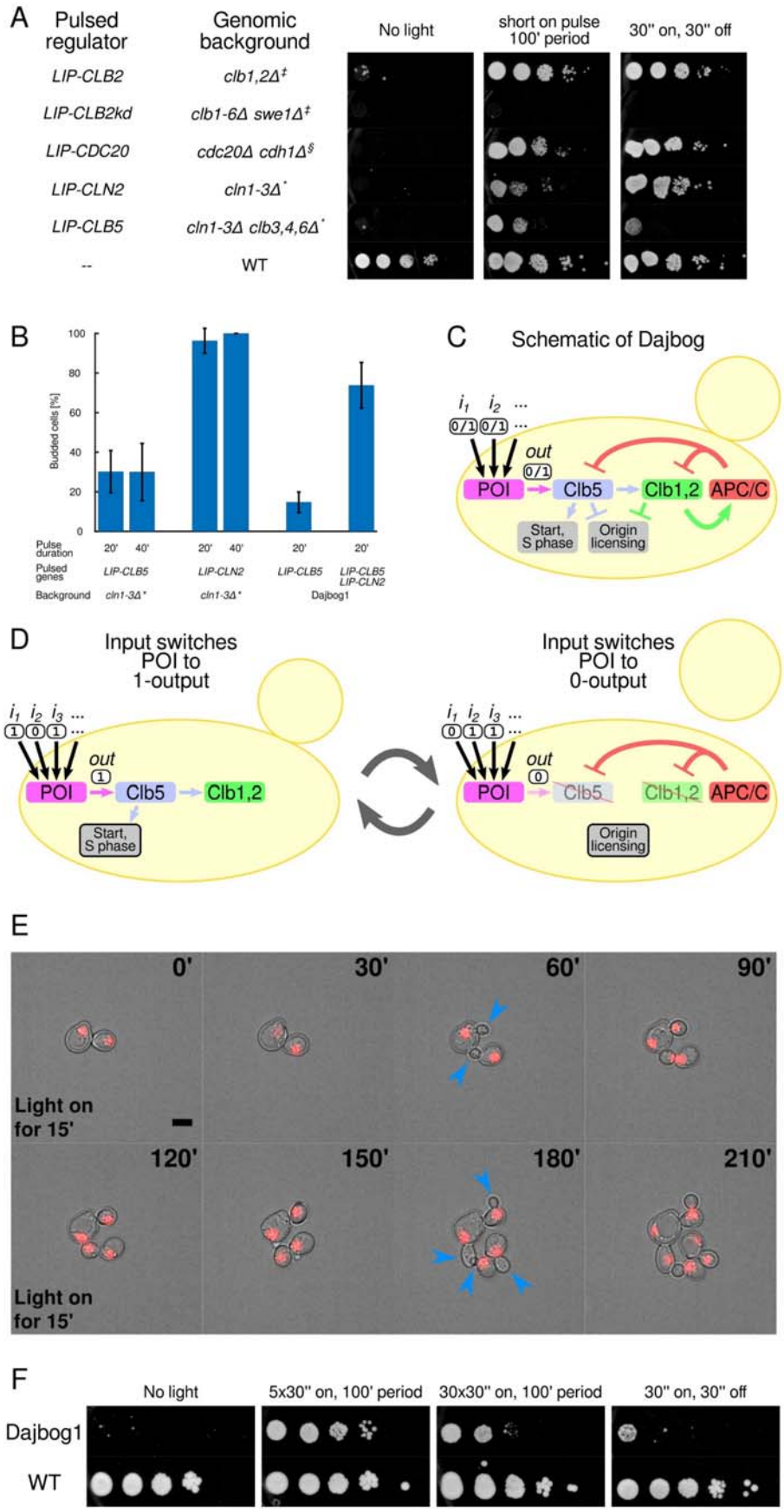
A
Pulsed regulator
Genomic background
No light
short on pulse 100' period
30'' on, 30'' off
LIP-CLB2
clb1,2Δ‡
LIP-CLB2kd
clb1-6Δ swe1Δ‡
LIP-CDC20
cdc20Δ cdh1Δ§
LIP-CLN2
cln1-3Δ*
LIP-CLB5
cln1-3Δ clb3,4,6Δ*
--
WT
B
Budded cells [%]
Pulse duration
Pulsed genes
Background
LIP-CLB5
LIP-CLN2
LIP-CLB5
LIP-CLB5 LIP-CLN2
cln1-3Δ*
Dajbog1
C
Schematic of Dajbog
POI
Clb5
Clb1,2
APC/C
out
Start, S phase
Origin licensing
D
Input switches POI to 1-output
Input switches POI to 0-output
E
0'
30'
60'
90'
120'
150'
180'
210'
Light on for 15'
F
No light
5x30'' on, 100' period
30x30'' on, 100' period
30'' on, 30'' off
Dajbog1
WT

269

Figure 2. Engineering budding yeast strains for optovolution. A: Initial tests of different cell cycle regulators with respect to three properties: essential for proliferation (cells inviable when regulator is off), sufficient for proliferation when pulsed (5 light pulses of 30 sec on, 30 sec off administered every 100 min, except for *cln1-3Δ clb3,4,6Δ* we used 30 such light pulses), and lethal when expressed continuously (30 sec on, 30 sec off). All cells expressed *EL222*, which induces *LIP*. Spot tests were performed with ten-fold dilutions. (Note that panel F shows tests for the Dajbog1 strain, which has been improved with respect to these desired properties.) B: Efficiency of cell cycle initiation (budding) when different light-inducible cell cycle regulators are activated, assessed by timelapse microscopy. Error bars show 5-95% confidence intervals. Number of scored cells are given in Supplementary Table 3. C: Schematic of cell cycle regulators in Dajbog strains. A subset of key cell cycle elements is shown only. Cln2 and Sic1 were omitted for clarity. D: Illustration of cell cycle states of the Dajbog strains when the POI output is on (1) or off (0). E: Timelapse recording of Dajbog1 strain, exposed to diascopic microscope light every 120 min for 15 min. Cells carry the red fluorescent nuclear marker Htb2-mCherry. Scale bar: 5 µm. F: Spot test of Dajbog1 strain under different light pulse regimes, revealing 5 times 30 sec on, 30 sec off every 100 min to be optimal among the conditions tested. Spot tests were performed with ten-fold dilutions. To keep cells proliferating before the tests, cells carried chromosomal constructs with chemical inducible *MET3pr-CLN2* (*), *GALL-CLB2* (‡), or *MET3pr-CDC20* (§), which were shut off during the tests by glucose or methionine in the agar plates.

The cell cycle regulators discussed thus far control mitotic transitions, where arrest and release often induce aneuploidy. We next shifted our focus to cyclins which control the G1-to-Start transition, which is less perilous for genomic stability. Parameters and response signatures of *CLN2* pulsing were extensively tested in ref.[129] However, again, constitutive over-expression of the G1/S cyclin *CLN2* from El222/*LIP* in the *cln1-3Δ* background, where *CLN2* is essential, did not kill cells. Thus, we turned to the S-phase cyclin *CLB5*. We first tested *LIP-CLB5* in a *cln1-3Δ* strain since *CLB5* expression is known to override a *cln1-3Δ* G1 arrest, although with lower efficiency than G1/S cyclin *CLN2*. In darkness, cells were arrested in G1. Light pulses with a 90 min period led to repeated cell cycles. Fortuitously, we found that constitutive *CLB5* expression by El222/*LIP* was lethal. (In contrast, *GAL1pr-CLB5* overexpression in galactose medium, as opposed to glucose medium, where cell cycles are substantially slower, is tolerated.) Thus, *CLB5* was a promising candidate for creating a tight coupling between the POI and the cell cycle. The system fulfilled requirement 1.

Next, we engineered the system for mutational robustness (requirement 2). To further increase the cells' dependence on *LIP-CLB5* expression, we deleted the four chromosomal *CLB3,4,5,6* genes, which can be functionally redundant with light-induced *CLB5*[130,131]. No mutations are known that can by-pass the requirement for Clb5 in a *cln1-3Δ clb3-6Δ* background.[132]

By deleting *CLB3-6* to make the strain even more strongly depend on *LIP-CLB5* induction, we could next also make the strain less tolerant to continuous *LIP-CLB5* expression. This would further increase the need for Clb5 to oscillate on and off for proliferation. We accomplished this by deleting *SIC1*, a B-type cyclin inhibitor. *SIC1* is part of a circuit that can oscillate when cyclin levels are constant and can rescue such cell cycles[127]. When *SIC1* is deleted, the *cln1-3Δ* arrest becomes

309 leaky[133]. However, we found that this depends on at least one of the *CLB3-6* genes being present.
310 *cln1-3Δ clb3-6Δ sic1Δ* cells continued to be tightly blocked in darkness.

311 The reliability of cell cycle initiation in response to a *LIP-CLB5* pulse was low (Fig. 2 B), violating
312 requirement 3. Only 30% of *cln1-3Δ* cells budded in response to a LIP-CLB5 pulse. In *cln1-3Δ*
313 *clb3,4,6Δ* cells, light-induced *LIP-CLB5* led to budding in even fewer (15%) G1-arrested cells. This
314 fraction was much higher (>90%) for *cln1-3Δ* cells with *LIP-CLN2*. Increasing the duration of the
315 light pulse did not change the fraction of *cln1-3Δ* cells that committed to the cell cycle. Guided by
316 these results, we sought to increase the reliability of the response to light pulses by adding a *LIP-*
317 *CLN2* construct. This does not undermine the dependence on *LIP-CLB5*, which continues to be
318 essential for S phase and triggering entry into mitosis in the *cln1-3Δ clb3-6Δ* background.
319 Simultaneous expression of *LIP-CLN2* and *LIP-CLB5* in the *cln1-3Δ clb3,4,6Δ* background led to a
320 more reliable >70% of cells budding in response to a 20 min pulse of light, satisfying requirement
321 3.

322 To enable routine propagation of these cells prior to directed evolution campaigns, we created a
323 'training-wheel plasmid' (requirement 4). This plasmid allowed cells to grow without exogenously
324 induced Clb5 oscillations, and the directed evolution campaign begins with counter-selection
325 against this plasmid. This increases the method's tolerance for POIs that initially cannot control
326 *CLB5* sufficiently well (requirement 5). We used a *URA3*-marked CEN/ARS plasmid, which can be
327 selected against with 5-FOA, containing a *CLB5* copy and *MET3pr-CLN2*. Finally, to increase the
328 mutation rate for directed evolution, we introduced the *pol3-L523D*[134–136] mutation that is
329 reported to increase the global mutation rate about one-hundred fold.

330 In summary, we achieved tight coupling of the cell cycle machinery to externally applied periodic
331 on-off light signals using Clb5 (aided by Cln2) in a *cln1-3Δ clb3-6Δ SIC1/sic1Δ* background (Fig. 2 C-
332 F). Clb5 triggered Start, S phase, and mitotic entry (Fig. 2 D). Simultaneously induced Cln2
333 substantially increased the fraction of cells initiating a cell cycle in response to a pulse of light.
334 Once Clb5 and Cln2 are no longer induced, they are degraded and diluted, allowing completion of
335 each cycle and resetting the cell state for a new cycle. In darkness or low light, cells arrested in G1.
336 Under constant light, cells could not proliferate as expected due to Clb5 blocking origin of
337 replication relicensing[137,138]. The poisonous effect of Clb5 can be enhanced by the *SIC1* deletion[139].
338 We further increased the mutation rate globally with the *pol3-L523D* mutation. Also, we allowed
339 the strain to proliferate without Clb5 oscillations using a training wheel plasmid until the start of
340 each directed evolution campaign. In principle, any POI controlling *CLB5* can be inserted for
341 directed evolution (requirement 5). In our tests, we never found strains to polyploidize, allowing
342 straightforward genetic analysis if needed (requirement 6). The strain fulfilled the requirements
343 for the continuous evolution of dynamic, multi-state, and computational protein functionalities.
344 We named the strain Dajbog2, and also used a variant with wild-type *SIC1* when more tolerance to
345 POI leakiness was required, which we named Dajbog1.[140]

346 ## Overview of directed evolution experiments

347 We performed five directed evolution campaigns with the Dajbog strains, in which we inserted
348 different POI genes to control cell-cycle progression. Cells initially proliferated on solid agar
349 growth medium plates under a permissive light pulse regime (Fig. 2). Then, for the start of the
350 directed evolution, cells were either spread on agar plates or suspended in liquid growth medium,
351 depending on the campaign. The desired selection pressure was imposed by changing to a
352 restrictive light pulse pattern under which the initial cells could not proliferate. We chose both
353 initial and final light pulse patterns without fine-tuning: Starting with the light pulse regime where
354 cells clearly proliferated well during strain construction, we chose a very different regime in which
355 cells obviously died. The frequency of mutations from standing variation, error-prone DNA
356 replication, and additional exposure to 10 sec of UV sufficed to find desired mutations in every
357 campaign (**Supplementary Table 4**).

358 On agar plates, mutant colonies emerged after 2 days and were then analyzed. At the end of the
359 liquid culture evolution experiment, we analyzed the bulk cell culture. Because optovolution
360 requires no changes in medium, cells remained on the same agar plate or, for the liquid culture
361 experiments, were diluted twice per day into fresh medium to maintain log phase.

362 ## Validation of mutants

363 We functionally validated the mutations *in vivo*: We cloned all mutations that emerged and
364 introduced them in wild-type budding yeast cells where the POI drove the transcription of the
365 bright, yeast-optimized *yEVenus* or *ymScarletI* fluorescent protein genes (**Methods**). We followed
366 the characterization procedure of ref.[88], using degron-destabilized fluorescent proteins for
367 dynamic timecourse measurements, fluorescence microscopy for relatively high accuracy, and
368 unbiased neural network-based image processing[141]. All fluorescence levels are expressed in
369 maxGAL1 units, an intuitive, easy-to-communicate unit for transcription.

370 Crucially, potential mutations elsewhere in the genome of the Dajbog cells, which could have
371 emerged in the directed evolution campaign, could not affect our characterizations of the
372 mutations. We thus established the causal effects of the evolved mutations independently of their
373 ability to support proliferation under the restrictive light pulsing regime in the Dajbog strains.

374 ## Directed evolution of a LOV-transcription factor

375 We first applied the method to optogenetic systems, i.e., the POI itself was light sensitive.
376 Optogenetic systems relay external on (1) or off (0) light states to on (1) or off (0) cellular activity,
377 i.e., they have two input-output relationships. Optogenetic systems have been challenging to
378 evolve, requiring repeated, sequential campaigns for the on (1) and off (0) output states since
379 mutations improving one output state may destroy the other.[142] Given that El222 is itself widely
380 used and that LOV domains are of broad interest, we chose to evolve El222 in three different

381 directions, toward i) greater light sensitivity, ii) less leakiness, or iii) different excitation spectra for
382 multiplexing and reduced phototoxicity.

383

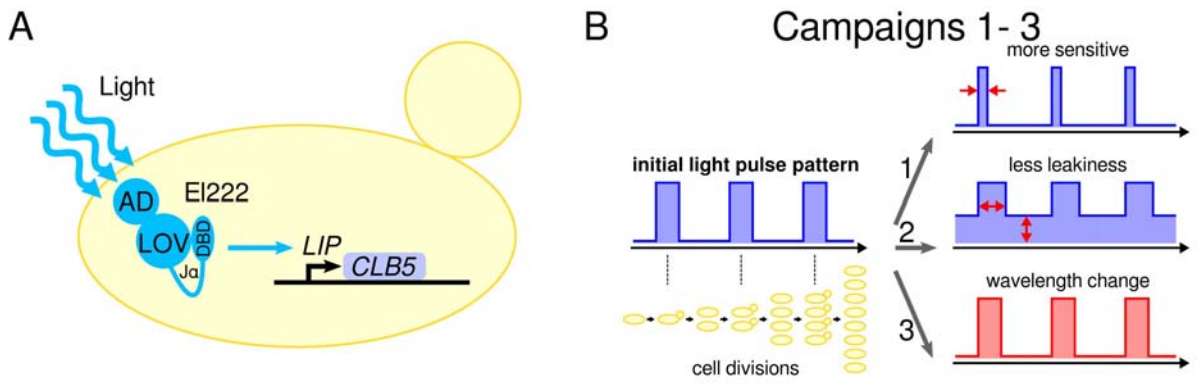

384

385 Figure 3. Directed evolution campaigns 1-3 with LOV-transcription factor El222 as POI. A. Schematic of the wiring
386 diagram for El222 evolution. *CLN2* and other cell cycle regulators omitted for clarity. AD, activation domain; LOV, LOV
387 domain; Jα, Jα helix; DBD, DNA binding domain. B. Schematic of three directed evolution campaigns. The initial light
388 pulse pattern was switched to 1) very brief pulses, 2) long pulses with additional ambient light, or 3) green and red
389 light pulses. Under each final light pulse regime, wild-type Dajbog cells did not proliferate.

390

391 We used the Dajbog strains with El222 directly controlling *CLN2* and *CLB5* transcription in the
392 same configuration as for testing and developing our method (Fig. 3 A). Cells initially proliferated
393 under a permissive light pulse regime (5 times 25 sec on, 35 sec off every 100 min). Then, we
394 changed the light pulse regime to apply one of three specific selection pressures, in which cells
395 with wild-type El222 could not proliferate (Fig. 3 B). (See Supplementary Fig. 1 for the excitation
396 and imaging light spectra.)

397 In the first directed evolution campaign, we sought to enhance the 1-output (on) state of El222.
398 This would allow higher output under low light conditions. To evolve more light-sensitive mutants,
399 we exposed cells to very brief light pulses (1 sec on every 100 min, Fig. 3 B), which was insufficient
400 for viability of the Dajbog cells initially. In the colonies that grew under these conditions (Fig. 4 A),
401 we found 11 different El222 mutations (Fig. 4 B). Remarkably, using Dajbog2 (with *sic1Δ*) we
402 observed 96% (n = 247) of colonies had a mutation in *EL222* while Dajbog1 (with *SIC1*) permitted
403 mutations elsewhere in the genome to rescue cells (10% in *EL222*, n = 816). Evaluating the new
404 El222 variants cloned into our reporter strain, we found that they showed improved light
405 sensitivity, with levels of transcription under low-intensity light up to 16 times higher than with
406 wild-type *EL222* (Fig. 4 B). Several variants were comparable or more light sensitive than the most
407 sensitive El222 mutant to date, strongLOV, which we had engineered previously[88].

408 To characterize the dynamic properties of the evolved El222 variants, we monitored their activity
409 by fluorescence timelapse microscopy where we induced them with diascopic light for 3.5 h (Fig. 4
410 C). All tested variants showed increased activity compared to wild-type El222 when using a

411 constant light source of 8.4 mW/cm^2. For most variants, we observed a trade-off between
412 strength and turn-off dynamics, similar to strongLOV[88]. However, remarkably, the highly light-
413 sensitive variant A157V, containing a mutation in the Jα helix, showed turn-off dynamics
414 comparable to wt-El222. (All references to mutant residue numbers in El222 are conventionally
415 given with respect to bacterial El222 to match the numbering used in previous work[88,143,144]).

416 This mutant is further interesting because it is the only one outside the LOV domain of El222 (Fig.
417 4 D). Within the LOV domain, the Fα helix, which is adjacent to the chromophore, was particularly
418 enriched for light-sensitizing mutations.

419

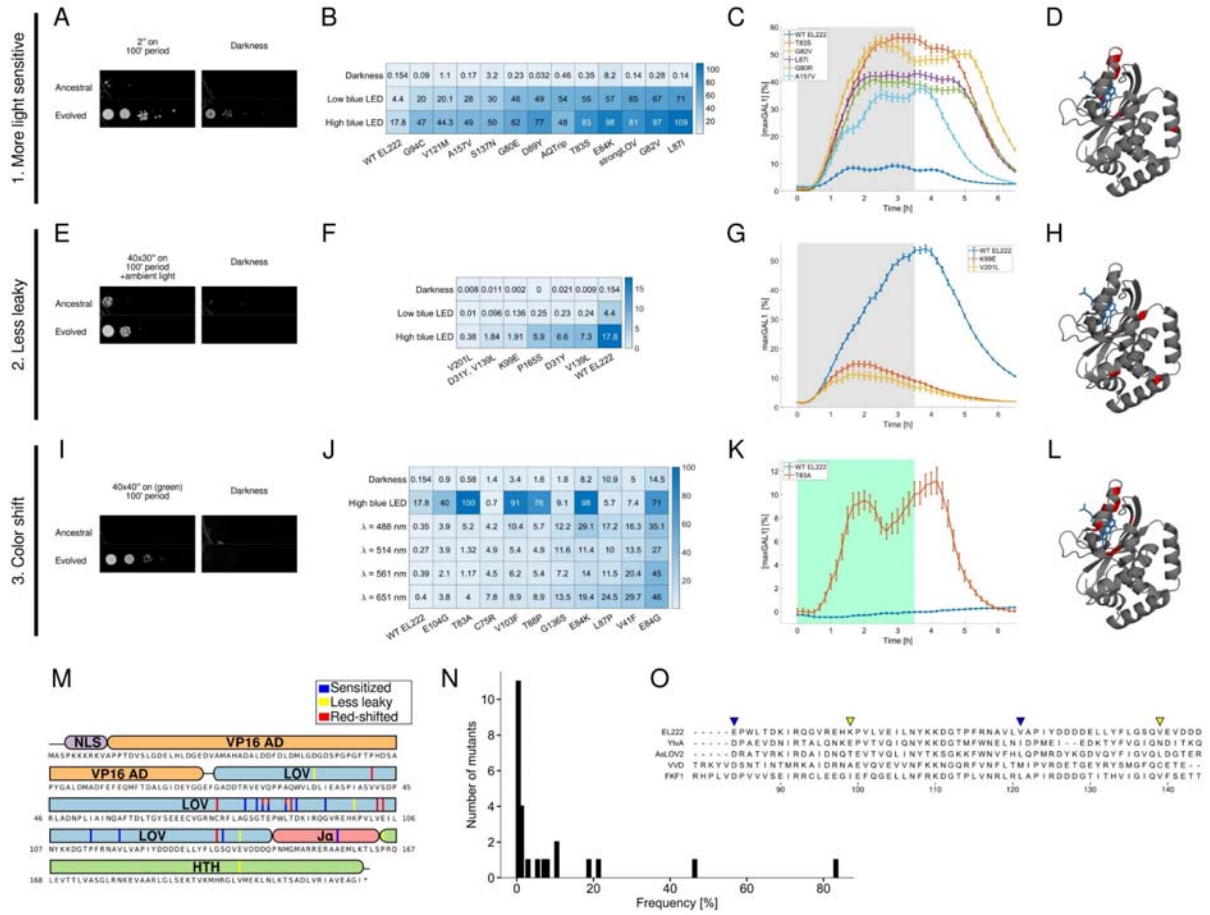

420

421 Figure 4. Results of three directed evolution campaigns of El222. Directed evolution for higher light sensitivity (A-D),
422 lower leakiness (E-H), and color shift (I-L). Panels A, E, I represent spot tests for the wild-type Dajbog strain (ancestor)
423 and typical mutants (evolved) that emerged in the different campaigns. Spot tests were performed with ten-fold
424 dilutions. Panels B, F, J show *in vivo* steady-state expression levels of the transcriptional fluorescent reporter *LIP-*
425 *yEVenus* under different light exposure conditions, driven by mutant *EL222*, which has been cloned from the Dajbog
426 strains and introduced into the reporter strain. All values are in maxGAL1 units[88]. In panel B, we included AQTrip[144] for
427 reference. C, G, K show timecourses of some of the El222 mutants we characterized, driving a destabilized fluorescent
428 transcriptional reporter with PEST degron. The optogenetic systems were induced from 0 h to 3.5 h by diascopic light
429 (C, G) or with an additional green filter inserted into the light path (K) as indicated by the highlighted regions[88]. Error
430 bars show the standard error of the mean around each timepoint. Panels D, H, L depict the locations of the mutations

431 (red) in the dark-state 3D structure of El222 (PDB ID: 3P7N)[143]. M: Positions of mutations in the domain diagram of
432 El222. N: Histogram of the frequency with which the mutations from our three campaigns are found in putative LOV
433 domains identified in ref.[145]. O: Searching for the mutations from our three campaigns in LOV domains with
434 characterized dark-reversion kinetics[89] (FKF1 from *Arabidopsis thaliana,* VVD from *Neurospora crassa,* YtvA from
435 *Bacillus subtilis,* and the LOV2 domain of phot1 from *Avena sativa*) identifies the light-sensitizing V121M and
436 strongLOV (E84D) mutations (blue arrows) and the mutations K99E and V139L (yellow arrows), which reduce
437 leakiness. All references to mutant residue numbers in El222 are given with respect to bacterial El222 to match the
438 numbering used previously[88,143,144]. B, C, F, G, J, K: Numbers of analyzed cells are given in Supplementary Tables 5-8. All
439 measured characteristics of the new El222 mutants have been added to the Inducible Transcriptional Systems
440 Database (https://promoter-benchmark.epfl.ch/)[88].

441

442 In the next campaign, we sought to reduce the leakiness of El222, that is, suppress activity in the
443 0-output (off) state. This is particularly important for applications where baseline expression needs
444 to be minimized, e.g., when controlling toxic genes. We exposed cells to very long duration pulses
445 of light (40 times 30 sec on, 30 sec off every 100 min, Fig. 3 B) in addition to continuous, dim
446 background light (Fig 4 E-H). This condition was lethal to Dajbog strains with wt-El222 (Fig. 4 E). In
447 a preliminary run, we found many mutations in *LIP-CLB5*, which presumably maintained Clb5
448 function but with reduced activity that blunted the selection pressure. Thus, we introduced
449 additional copies of *LIP-CLB5* to block this evolutionary avenue (**Discussion**). Among the mutant
450 colonies that emerged in this campaign, the frequency of mutations in the *EL222* ORF was 36% (n
451 = 44).

452 We identified five new mutations whose leakiness was nearly indistinguishable from baseline
453 transcription from *LIP* in the absence of El222 (Fig. 4 F, Supplementary Fig. 2). As expected, they
454 were also overall less strongly induced by light. One of the colonies that emerged had fixed two
455 mutations in the LOV domain (D31Y, V139L). To understand their individual contributions to the
456 phenotype, we tested them separately. The mutations contributed independently and about
457 equally under high blue LED light. We also measured the on-off dynamics of low-leakiness mutants
458 by fluorescence microscopy. Using continuous light of 8.4 mW/cm^2 as in the case for light-
459 sensitized mutants led to no observable activity in the low-leakiness mutants (not shown). Under
460 stronger light (97 mW/cm^2), the mutants responded at 20% of wt-El222 output (Fig. 4 G). The low-
461 leakiness mutations were both in the LOV domain as well as the DNA binding domain (Fig. 4 H).

462 In our third campaign, we sought to modify the nature of the 1-output state with respect to color
463 responsiveness. After proliferating Dajbog cells under blue light pulses, we evolved them under
464 green, orange, and red light combined (40 times 30 sec on, 30 sec off every 100 min). (Figs. 3 B, 4
465 I-L, Supplementary Fig. 1 for details regarding light sources). Among the mutant colonies that
466 emerged, we discovered numerous mutations in *EL222* that allowed cells to proliferate under
467 green-to-red light pulses. Optovolution was highly efficient: 96% (n=247) of mutations were in the
468 *EL222* ORF when Dajbog2 (with *sic1Δ*) was used and 10% (n = 816) with Dajbog1 (with *SIC1*).

469 Again, we validated the mutations functionally by cloning the evolved *EL222* genes into the
470 reporter strain. Since the green LEDs that we used for directed evolution had an emission
471 spectrum that extended below 500 nm (Supplementary Fig. 1), which overlaps with the excitation
472 spectrum of wt-El222[143], we excluded merely light-sensitized mutants with a 514 nm laser. Ten
473 El222 mutants activated the transcriptional reporter substantially when excited by a 514 nm laser
474 (Supplementary Fig. 3). We focused only on these mutants and disregarded the others. To
475 measure the *in vivo* action spectrum of the mutant El222s, that is, the relationship between the
476 wavelength of excitation light and the level of activity, we used additionally blue 488 nm, yellow
477 561 nm, and red 651 nm lasers (Fig. 4 J). To detect the sensitivity to each wavelength and not
478 saturate the on (1) state of the transcription factors, we set the lasers to relatively low average
479 power (3.5 mW/cm^2 delivered over 6 h), which was enough to induce all of the color-shifted
480 mutants. We also included as a reference the blue LED light used for characterization of the
481 previously described sensitized and low-leakiness variants (Fig. 4 B, F). The measurements showed
482 that the mutated El222 variants were not only responsive to green but also to red light (Fig. 4 J). In
483 fact, red 651 nm laser light generated comparable or even stronger responses from our color-
484 shifted El222 variants. Some of the variants responded to red light much more strongly than wild-
485 type El222 to blue light but were also more leaky. The largest dynamic range we observed was
486 7.5x for the G136S mutant. Surprisingly, under blue light of high intensity, some of the mutants
487 (C75R, G136S, L87P, and V41F) showed a lower level of activity compared to blue or red laser light
488 of low intensity. We characterized the dynamics of one red-responsive *EL222* mutant using
489 fluorescence timelapse microscopy and the *LIP-ymScarletI-PEST* reporter (Fig. 4 K).

490 Unlike for the light-sensitized and low-leakiness variants, the red-shifting mutations clustered
491 tightly around the chromophore (Fig. 4 L). Interestingly, one of the red-responsive variants had an
492 arginine residue instead of the critical Cys-75 residue that forms a covalent bond with the
493 chromophore after exposure to blue light[146]. In *in vitro* experiments, LOV domains without this
494 strictly conserved cysteine were previously shown to incorporate a partially reduced flavin
495 chromophore[147], pointing to one potential explanation for our color-shifted El222 mutants.

496 In total, we discovered 25 mutations, mostly in the LOV domain, one in the Jα helix, and two in the
497 DNA binding domain (Fig. 4 M). The analysis of the mutation spectrum in the first three campaigns
498 showed that we observed transitions and transversions with about equal probability
499 (**Supplementary Table 4**).

500 LOV domain proteins such as El222 are ubiquitous across the tree of life and control a variety of
501 cellular processes. Most approaches to altering LOV-optogenetic tools have involved introducing
502 mutations from other known natural LOV domains, which were faster or slower cycling[87,89,144]. To
503 gauge how realistic it would have been to discover our evolved mutants rationally, we first
504 quantified the novelty of our mutants by searching a catalog of 7000 known and putative LOV-
505 domains (Fig. 4 N) as well as by aligning their sequences with the well-studied LOV-domain
506 proteins FKF1 from *Arabidopsis thaliana*, VVD from *Neurospora crassa*, YtvA from *Bacillus subtilis*,

507 and the LOV2 domain of phot1 from *Avena sativa* (Fig. 4 O). We discovered that the majority of
508 the mutations (21/25) were rare (≤10%) in putative LOV domains, and 4 are present in LOV
509 domains whose kinetics had previously been characterized. V121M found in VVD is part of the
510 rationally-designed El222 variant AQTrip[144]. Similarly, another mutation (E84D) was used to
511 construct the more light-sensitive strongLOV mutant protein by us recently (Fig. 4 O, blue
512 triangle)[88]. Interestingly, the other two mutations, K99E and V139L (Fig. 4 O, yellow triangles),
513 would have been expected to lead to more stable light-adapted states based on previously
514 measured off-kinetics[87]. We found them, instead, to lead to lower leakiness and overall weaker
515 responses. These results further underscore the power of directed evolution to uncover functional
516 mutations with specific desired properties.

517 Long-term optovolution of light-sensitized LOV domains

518 The directed evolution campaigns described thus far were unbiased by design: Any El222 mutant
519 which emerged and which could switch on and off repeatedly for ≈2 days under the respective
520 selection pressure would generate a colony and be detected by us. Next, we wished to test
521 whether optovolution could be used for directed evolution over longer periods of time in liquid
522 culture, where mutations could compound and compete against one another. The fittest mutant
523 would take over the cell culture.

524 We again sought to boost the 1-output activity of El222, this time over one week (**Methods**). We
525 evolved the Dajbog2 strain under 5 sec of light, administered every 100 min. We observed two
526 mutations that won in two different long-term experiments, E84D and V121M, which we had
527 already discovered using the previous unbiased approach.

528 Directed evolution of the PhyB-Pif3 system independent of exogenous 529 chromophore

530 In our next evolutionary campaign, we wished to improve the usability of the red-/far-red-light
531 controlled optogenetic switch PhyB-Pif3. For this purpose, we put *CLN2* and *CLB5* under the
532 control of the *GAL1* promoter and introduced *ADH1pr-PHYB-GAL4BD* and *ADH1pr-GAL4AD-PIF3*
533 constructs. (Fig. 5 A). We screened for mutations allowing cell proliferation without supplementing
534 PCB (Fig. 5 B). In three out of three mutants sequenced, we found mutations in the *YOR1* (also
535 known as *YCF1*) gene, two of which were early nonsense mutations (Q64*, E421K, E1318*). Yor1 is
536 a plasma membrane exporter[148], a homolog of human cystic fibrosis transmembrane receptor
537 (CFTR)[149].

538 We validated that a *YOR1* deletion suffices to remove the need to supplement PCB for PhyB-Pif3
539 function in two reporter strains from other laboratories. We deleted *YOR1* in a strain from ref.[110],
540 in which PhyB-Pif3 drives the transcription of a fluorescent reporter (Fig. 5 C). In the absence of
541 PCB, the fluorescent reporter in the strain with *YOR1* deletion responded similarly as with PCB in
542 the presence of *YOR1*. Leakiness was comparable with and without *YOR1*. Since PhyB-Pif3 is

543 frequently used to control localization of proteins to different cellular compartments, we tested
544 that *yor1Δ* sufficed to replace supplemental PCB for this purpose as well. We deleted *YOR1* in a
545 yeast strain from ref.[150] in which PhyB is anchored to mitochondria, labeled with mCherry, and Pif3
546 is fused to a yellow fluorescent protein and Bem1 (PhyB-mCherry-Tom7, Bem1-mCitrine-Pif3).
547 Exposing the *yor1Δ* version of this strain to red light led to colocalization of PhyB and Pif3,
548 indicating their interaction (average per-cell Pearson correlation for yellow and red fluorescence r
549 = 0.60, N_cells = 21). As a control, we tested the colocalization of PhyB and Pif3 in the *yor1Δ* strain
550 with PCB, which led to r = 0.73 (N_cells = 32). In wt-*YOR1* cells, we observed low colocalization (r =
551 0.25, N_cells = 17), while the addition of PCB showed localization comparable to *yor1Δ* without
552 PCB (r = 0.78, N_cells = 31).

553

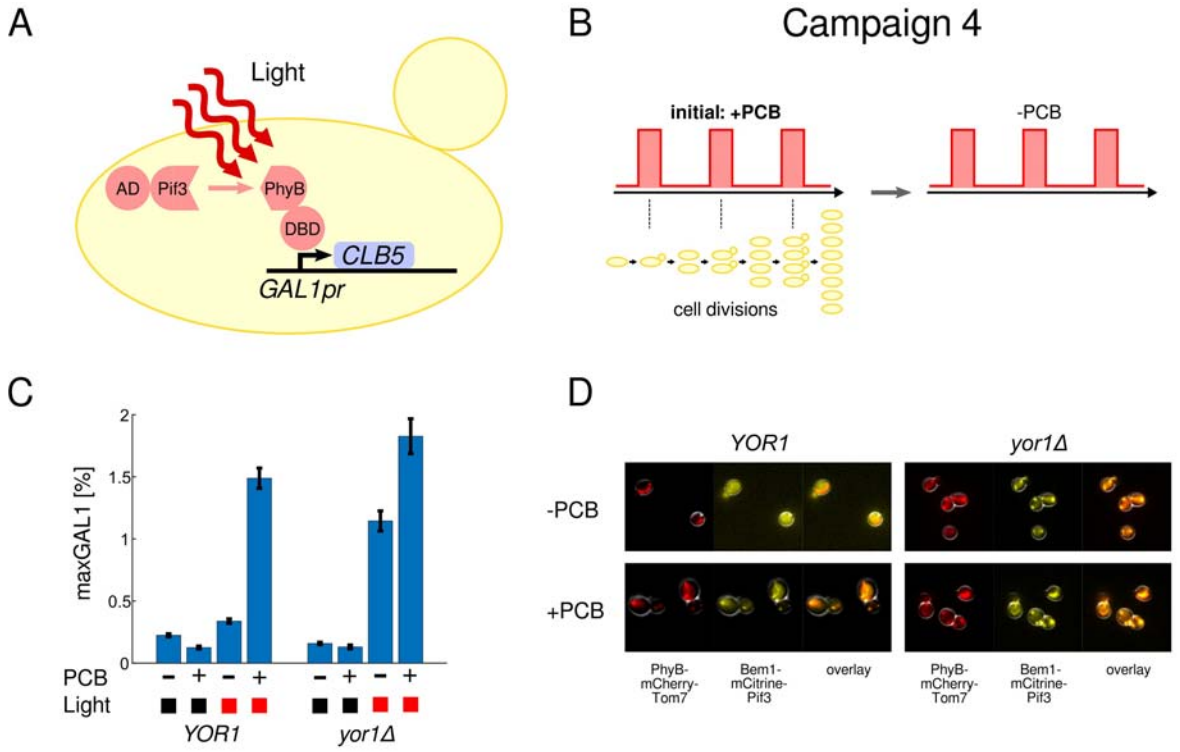

554
555 Figure 5. Directed evolution campaign 4 to lose the dependence of PhyB-Pif3 on supplemental PCB. A: Schematic of
556 the wiring diagram relevant for the campaign. (*CLN2* and other cell cycle regulators omitted for clarity.) AD, activation
557 domain; DBD, DNA binding domain. B: Schematic of the campaign. C: *GAL1pr-yEVenus* induction with or without *YOR1*
558 deletion, which was identified in this campaign. Error bars represent standard error of the mean. Numbers of analyzed
559 cells are given in Supplementary Table 9. D: Test of co-localization of Pif3 to mitochondrially anchored PhyB with or
560 without *YOR1*. The PCB concentration was 10 µM where supplemented. The measured characteristics of PhyB-Pif3
561 with and without *YOR1* have been added to the Inducible Transcriptional Systems Database (https://promoter-
562 benchmark.epfl.ch/)[88].

563

564 ## Directed evolution of a light- and doxycycline- inducible AND gate

565 In our fifth evolutionary campaign, we applied optovolution to a non-optogenetic system. First, we
566 engineered an AND gate based on the transcription factor rtTA, which is controlled by doxycycline.
567 To make rtTA dynamically sensitive to transcriptional input, we destabilized it by fusing its N-
568 terminus with a PEST degron. When *PEST-rtTA* was transcribed under the control of the El222/*LIP*
569 system, transcription from the rtTA-controlled promoter *tetOpr* was very weak.

570 We wished to evolve variants of the logic gate with stronger on (1) state activity. So, we
571 introduced *tetOpr-CLN2* and *tetOpr-CLB5* into the Dajbog1 strain (Fig. 6 A). We then evolved the
572 system by exposing cells to short pulses of blue light, 2 sec on every 100 min, under which they
573 could not proliferate (Fig. 6 B). Before evolution, light pulsing 30 times 30 sec on, 30 sec off every
574 100 min and doxycycline allowed cell proliferation, confirming the AND gate functionality prior to
575 directed evolution (Fig. 6 C). However, the *tetO* promoter is very leaky in budding yeast (*tetOpr-*
576 *yEVenus* expression was at 2% maxGAL1 without *rtTA*) so that even in darkness and without
577 doxycycline, Dajbog1 proliferated, albeit much more slowly. This is why we used the more
578 leakiness-tolerant Dajbog1 strain in this campaign and screened for mutants as soon as small
579 colonies emerged under 2 sec light pulses every 100 min.

580 In principle, mutations in any part of the system could lead to the increased activity. Given that we
581 have already extensively characterized the mutations that boost the activity of the El222/*LIP*
582 optogenetic system, we now focused on screening for mutations in *PEST-rtTA* (**Discussion**). We
583 discovered two mutations, F67C and R253H (numbering is with respect to +1 methionine in rtTA).

584 To characterize the *PEST-rtTA* mutants, we cloned and introduced them as single-copy constructs
585 driven by *PGK1pr* into a reporter strain with a single copy of *tetOpr-yEVenus-PEST* (Fig. 6 D). Both
586 mutations showed increased activity in the presence of doxycycline. The mutated residues are
587 located between the DNA binding domain and the rtTA core domain or in the VP16 transcriptional
588 activation domain, respectively (Fig. 6 E). Relatedly, in previous directed evolution experiments of
589 rtTA, F67S was identified as increasing the sensitivity of rtTA (without a degron) to doxycycline[151].

590 These results demonstrate how the light-driven selection pressure in optovolution can be
591 leveraged for the evolution of non-optogenetic proteins with dynamic, multi-state, and
592 computational properties.

593

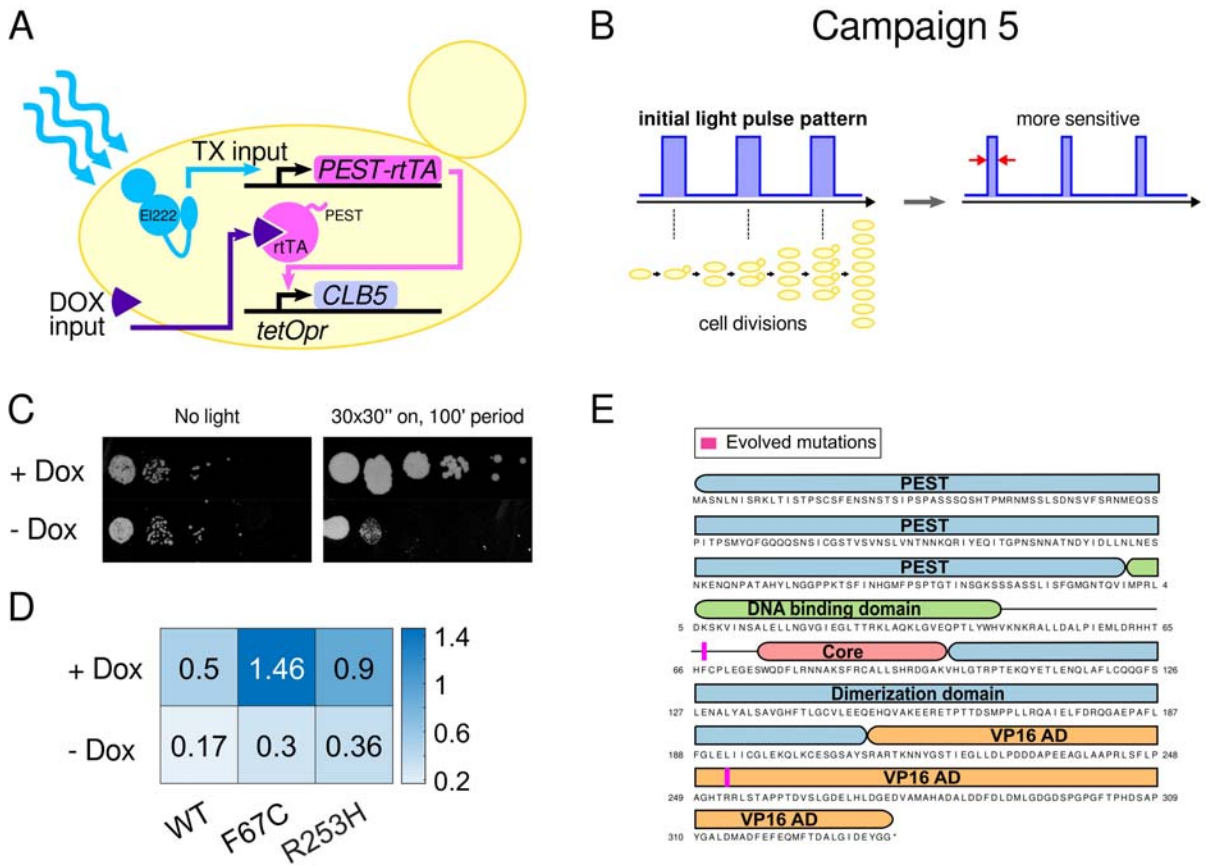

Figure 6. Directed evolution campaign 5 to improve the AND logic gate function of PEST-rtTA. A: Schematic of wiring diagram relevant for campaign. TX, transcription; DOX, doxycycline. B: Schematic of the campaign. C: Spot test for wild-type Dajbog1 strain with PEST-rtTA system with ten-fold dilutions. D: Expression level of *tetOpr-yEVenus-PEST* under the control of the original or evolved PEST-rtTA in maxGAL1 units. For lowering experimental variability, the original and mutant *PEST-rtTA* were expressed from the *PGK1* promoter. Residue numbers are with respect to +1 methionine of rtTA. Numbers of analyzed cells are given in the Supplementary Table 10. E: Positions of mutations in domain diagram of PEST-rtTA.

Discussion

Two key ideas underlying optovolution

The primary advance of our directed evolution paradigm is the coupling of the POI output to an element of cell cycle control that has to oscillate for cellular replication in the specially engineered Dajbog genetic background. This obviates interventions needed to screen phenotypes or to switch between selection mechanisms after each round of evolution. Instead, both 0-to-1 and 1-to-0 switching of the POI are effectively screened every ≈90 min by the cell cycle control machinery *in vivo*. In addition, the coupling of the desired POI properties to organismal fitness automatically ensures that the evolved variants are functional *in vivo*. Additional *in vitro* screening is not needed.

612 These advantages of our method arise from leveraging cell cycle control, to our knowledge, for the
613 first time for directed evolution.

614 Secondarily, we use optogenetics to cycle through the inputs of the POI. Fundamentally, light
615 control is powerful for directed evolution because it allows communicating with cells rapidly,
616 conveniently, and for extended periods. Thus, new kinds of selection pressures can be created,
617 which require dynamic interaction with cells. As far as we know, this is the first time that
618 optogenetics has been leveraged for continuous directed evolution.

619 Light control also allows straightforwardly shaping the fitness landscape of the POI by tuning the
620 selection pressure. Different evolutionary outcomes can be achieved depending on the light
621 exposure protocol. Input-output relationships can be challenged by administering light input that
622 is too weak or too strong. Directed evolution can be expected then to improve the input-output by
623 mutational adaptations. Similarly, engaging and releasing the POI early or late forces adaptations
624 toward improved POI kinetics. We used the same strain, with El222 directly controlling *CLB5* and
625 *CLN2*, for three different directed evolution campaigns: enhancement of the 1-output activity of
626 El222, suppression of the 0-output activity, or changing the excitation color. However, we only
627 used relatively simple light pulse patterns in this work, that is, we only modified the duration or
628 color of the light pulses (Figs. 3 B, 6 B). By tuning the light pulse parameters further or even
629 combining different pulse types, e.g., long-short-long-short-... light pulses, one may evolve yet
630 more variants of POIs, toward other desirable goals.

631 Tolerance toward poor initial POI functionality

632 A general challenge is that a POI may be so poor with respect to a desired function that the
633 directed evolution campaign cannot even be initiated. This is mitigated in two key ways in our
634 method: The selection pressure can be easily tuned by changing the light pulse regime, e.g.,
635 shorter, longer, dimmer, or brighter light pulses. In contrast, tuning of the selection pressure is not
636 straightforward in some continuous directed evolution approaches. Furthermore, the training
637 wheel plasmid allows proliferation in the absence of any POI function, so that directed evolution
638 of the POI can be initiated concomitantly with selection for loss of the training wheel plasmid on 5-
639 FOA.

640 Efficiency and targeted mutagenesis

641 Mutations in the POI gene evolved efficiently and by-pass mutations were either rarely observed
642 in Dajbog2 (*sic1Δ*) or were reasonable in number to quickly find the mutation of interest with
643 Dajbog1 (wt-*SIC1*). The strains can in principle be further optimized to suppress mutations in the
644 budding yeast genome. After identifying such by-pass mutations, one can effectively prevent them
645 by inserting additional copies of the gene. This strategy takes advantage of the tolerance of yeast
646 toward multiple copies of most of its genes[152,153] and the extremely low likelihood of mutations
647 occurring in different copies of the same gene. We demonstrated this strategy with multiple *LIP*-

648 *CLB5* copies in our second directed evolution campaign, also see **Extendibility of optovolution**.
649 Should by-pass mutations occur in non-essential genes, one can in principle simply prevent them
650 by deleting the gene.

651 The deep literature on cell cycle control can be used to guide future improvements of
652 optovolution. We leveraged the extensive genetic screens for suppressors of cell cycle arrest
653 performed in the past to create a genetically robust platform. Screens have only revealed *sic1Δ* to
654 by-pass *cln1-3Δ* arrest.[133] This by-pass relies on *CLB3-6*, which are absent in the Dajbog strains. (It
655 should be noted that *cln1-3Δsic1Δ* cells proliferate poorly, suggesting that by-pass mutations do
656 not necessarily affect directed evolution experiment in practice.) By-pass mutations in Cdk1 can be
657 practically ruled out since at least five mutations are required to run the cell cycle oscillator in a
658 *cln1-3Δ clb5,6Δ* background.[132] It is unknown whether even quintuply mutated Cdk1 could run the
659 Dajbog strains, which have additional deletions of *CLB3,4*.

660 Another potential way to increase the efficiency of our method is to take advantage of the
661 orthogonal advances that have been made to increase mutation rates specifically in genes of
662 interest. These are especially needed when mutations elsewhere in the genome can readily bypass
663 the desired POI functionality. However, Dajbog2 was genetically tight, so it was not necessary to
664 target mutations to the POI gene to achieve our goals. Furthermore, our campaigns succeeded
665 with 1-2 mutations, obviating or reducing the need to disentangle driver from passenger
666 mutations. Using *pol3-L523D*, we expected to increase the genome-wide mutation rate to 0.5×10^{-7}
667 per base-pair per generation. This means that in tens of milliliters of log-phase yeast population,
668 about all single mutants of the POI gene should have been present. Straightforward ways to
669 increase the mutation rates further globally involve the use of DNA damaging radiation and
670 chemicals, although not all nucleotide mutations can be attained in this manner. Another common
671 method to achieve very high rates of targeted mutations is to introduce the POI on mutagenized
672 plasmid libraries. Our method will also presumably benefit from combining with targeted *in vivo*
673 mutagenesis systems such as OrthoRep[10], MutaT7[12,154], or Cas9-[155] or transposon-mediated
674 systems[17].

675 Extendibility of optovolution

676 In addition to incorporating targeted mutagenesis, optovolution can be adapted for different
677 directed evolution goals using standard methods of yeast genetics and decades of research in
678 growth, metabolism, and cell cycle control:

679 1. The carbon source can be varied to slow down the cell cycle and growth to match POIs that
680 switch poorly. The carbon source can then be changed for faster cycling as the POI switching
681 kinetics improves during directed evolution.

682 2. Restoring *SIC1*, which makes the system less sensitive to residual Clb5, allows POIs to be
683 evolved that are initially more leaky.

684 3. In principle, POIs can be elements of multi-step signaling cascades (optogenetics → POI →
685 Clb5,Cln2) involving mediators and transducers as we showed for PEST-rtTA. Undesired mutations
686 can occur in this cascade outside the POI gene, irrespective of the genetic robustness of the
687 Dajbog strains. These outcomes can be suppressed similar to potential genomic by-pass
688 mutations. All elements of the pathway can straightforwardly be introduced in multiple copies.
689 (Whether the POI gene should be inserted in single or multiple copies depends on the goal.) We
690 used this method in campaign 2 to suppress by-pass mutations in *LIP-CLB5*. We would have
691 utilized it in campaign 5 if mutations in *EL222* would have overwhelmed new mutations in *PEST-*
692 *rtTA*, which was not the case in our experiments.

693 4. A number of degrons can be added to reduce the activity of a POI[156].

694 5. Given that control of Clb5 is the key element of optovolution, the method is in principle
695 extendable to POIs that control Clb5 activity in other ways than transcription. However, we did not
696 specifically demonstrate this possibility here. Use of the more stable destruction-box deficient
697 Clb5db opens up additional such options[139,157,158].

698 6. Chemically controlled POIs that can regulate Clb5 activity are in principle fully compatible
699 with the Dajbog strains. In fact, past non-continuous directed evolution methods used
700 transcriptional POI output for selection/counterselection cycles, which suits well the need to
701 control *CLB5* and *CLN2* in the Dajbog strains. For chemical POI inputs, cell culture media generally
702 would have to be switched to cycle through different inputs, making evolution non-continuous. By
703 using the Dajbog strains, cell cycle control would continue to be the dynamic selection mechanism,
704 which is the essential novelty of our method. Thus, the chemicals otherwise needed for
705 selection/counter-selection, e.g., -uracil versus +5-FOA, would not need to be exchanged. This may
706 facilitate speed-up of selection/counterselection cycles to ≈1.5 hrs versus 2 to 5 days in past
707 campaigns with yeast – if the media exchanges can be performed sufficiently quickly.

708 Limitations of optovolution

709 Limitations on types of POI input: Our directed evolution of PEST-rtTA demonstrated that the POI
710 itself need not be light sensitive. Options for light control of the POI are diverse and rapidly
711 expanding, including light-controlled transcriptional input (used for PEST-rtTA), light-controlled
712 protein-protein interaction (used for PhyB-Pif3), light-controlled degrons, kinases, and mRNA
713 targeting systems. POIs that can only be controlled with chemicals are compatible with our
714 platform but would require intervention, albeit only to cycle through the POI inputs.

715 Limitations on types of POI output: We demonstrated optovolution by evolving POIs that control
716 the transcription of *CLB5*: two transcription factors, El222 and PEST-rtTA, and an inducible protein-
717 protein interaction system, PhyB-Pif3, which was repurposed to control transcription using the
718 yeast two-hybrid system. Many existing continuous directed evolution methods[14,34,35] were
719 similarly initially applied to POIs that control transcription, presumably because transcriptional

control can be created in a multitude of ways: The well-established two-hybrid method, which the PhyB-Pif3 transcriptional system is based on, converts protein-protein interactions into transcriptional output[159]. CRISPR-Cas systems were in many cases evolved by blunting the endonuclease activity of Cas proteins and coupling to transcriptional output.[25,26,160,161] GPCRs were similarly screened by coupling downstream signaling to transcription.[162–164] Thus, transcriptional control of *CLB5* does not limit the POI to transcription factors. Furthermore, the crucial element of our method is control of Clb5 activity, which can in principle be coupled to POI activity in other ways.

Limitations on targeting POIs: Even if the cell cycle-coupled selection mechanism is genetically robust, genomic mutations can emerge that are in cellular pathways affecting POI function. An example in our study is *YOR1*, whose mutations allowed PhyB-Pif3 to respond to red light in the absence of PCB. We considered the mutations in *YOR1* to be sufficiently surprising and useful to report in their own right as an endpoint of that campaign, instead of seeking to suppress them.

Requirement of minimal computational functionalities: Optovolution is fundamentally not suited for proteins whose state switching cannot be controlled even by way of intermediates, or for proteins that cannot control Clb5 activity. Essentially, the POI must meet the minimum requirements for computational functionality: controllable inputs and an output that can be read out, specifically, by coupling to Clb5. For example, proteins that stochastically switch between states without input or that are not coupled to an activity that could ultimately control Clb5 are not evolvable with optovolution.

Outlook for evolving computational functionalities

Given the appropriate selection pressure, directed evolution can solve challenging engineering problems and uncover unexpected solutions -- such as red-responsive El222 mutants or PCB independence conferred by *yor1Δ*. Here, we present the first method for continuous directed evolution of dynamic, multi-state, and computational protein functionalities. Such capabilities are fundamental to signal transduction -- and thus to life. While much of cellular biochemistry computes decisions, it had been unclear how continuous directed evolution could be adapted to such capabilities. Apart from interest in this as a fundamental problem, a solution is also needed for biological engineering since dynamic, multi-state, and computational properties are of intense current interest, especially, in protein design[165–169].

More advanced computational capabilities involve more inputs for more complex input-output relationships. Using optovolution, different colors (UV[170,171], blue[103], green[172], red[108,173]) and optogenetic systems allow administering different inputs to the POI and cycling through input combinations during evolution.[99–102,172,174,175] The number of optogenetic effectors is steadily increasing, enabling different kinds of input to the POIs[176]. Single-protein computers would have numerous advantages over multi-gene circuits, including simpler genetic introduction into cells and presumably faster kinetics. However, rational engineering of proteins often leads to poorly

757 performing molecules, e.g., the initially engineered AND gate PEST-rtTA in this work, underscoring
758 the need for directed evolution approaches.

759 Optovolution is particularly timely for the revolution that is currently taking place in artificial
760 intelligence-based protein design, in which there is substantial interest in dynamic, multi-state,
761 and computational properties[29,177–179]. Prototypes that have been computationally designed can
762 be screened and improved in a high-throughput manner with optovolution. Additionally, machine-
763 learning guided methods will keep relying on experimentally validated training sets, which can be
764 further enriched through directed evolution. We expect optovolution to provide solutions to
765 previously intractable engineering problems and pave the way for more sophisticated proteins.

766

767 # Methods

768 ## Media

769 We used synthetic complete media[180] (SCD) with methionine (+Met) or without methionine (-Met)
770 and supplemented with 2% (w/v) glucose. For preparing solid SC plates, we used 2% agar. For
771 experiments with 5-FOA, we used a standard recipe with 0.1% 5-FOA[71,181]. For controlling and
772 evolving the transcriptionally and doxycycline-regulated AND gate (PEST-rtTA), we used 30 µM
773 doxycycline diluted from a 1000x stock in water (Sigma, USA). For characterization of the PEST-
774 rtTA variants, we used 10 µM doxycycline. For experiments with PhyB-Pif3, we used 10 µM PCB,
775 diluted from a 1000x DMSO stock (Sychem, Germany) when supplying exogenous PCB.

776 ## Plasmid construction

777 Cloning was performed using restriction enzyme digestion and ligation with T4 ligase (New
778 England Biolabs) or Gibson assembly (New England Biolabs). Plasmids were propagated in
779 DH5alpha *E. coli* in LB medium supplemented with ampicillin. See Supplementary Table 1 for a list
780 of the plasmids.

781 ## Strain construction and preparation for directed evolution

782 Transformations of budding yeast were performed using the high-efficiency LiAc/DNA carrier/PEG
783 (polyethylene glycol) protocol[182]. All strains are derivatives of W303 (*leu2-3,112 trp1-1 can1-100*
784 *ura3-1 ade2-1 his3-11,15*). A list of strains is provided in Supplementary Table 2.

785 The Dajbog1 (*cln1-3Δ clb3-6Δ*) and Dajbog2 (*cln1-3Δ clb3-6Δ sic1Δ*) strains proliferated in the
786 absence of light pulses in SCD-Met medium plates due to the presence of the *URA3*-marked
787 training wheel plasmid pRD-TW1 (*MET3pr-CLN2, CLB5pr-CLB5, CEN/ARS*), which was built using
788 pRS416[183]. (Lack of methionine induces *MET3pr-CLN2*.) For the different directed evolution
789 campaigns, we built additional strains starting with the Dajbog strains. To evolve *EL222* (first three
790 campaigns), we transformed the strains with *LIP-CLB5*, *LIP-CLN2*, and *PGK1pr-EL222* constructs.
791 For the evolution of the PhyB-Pif3 system (fourth campaign), we transformed them with *ADH1pr-*
792 *PHYB-GALBD*, *ADH1pr-GAL4AD-PIF3*, *GAL1pr-CLN2*, and *GAL1pr-CLB5* constructs. Lastly, for
793 evolving the AND gate (fifth campaign), we transformed the strains with *PGK1pr-EL222*, *LIP-PEST-*
794 *rtTA*, *tetOpr-CLN2*, and *tetOpr-CLB5*. We confirmed transformations by PCR.

795 To prepare the strains for directed evolution experiments, we selected for the loss of the training
796 wheel plasmid as follows: First, cells were spread on fresh SCD+Met plates and placed under
797 pulsing light. Methionine shuts off *MET3pr*, reducing any advantage that the training wheel may
798 confer and thus increasing the fraction of cells that lose the training wheel plasmid. Then, we
799 transferred cells to SCD+Met+5-FOA plates under the same pulsing light regime, so only cells that
800 had lost the training wheel plasmid could proliferate. We picked isolated colonies in which we

801 confirmed the loss of the training wheel plasmid by the lack of growth in darkness on plates
802 lacking methionine. From then on, the strains were propagated under pulsing light.

803 After directed evolution, we characterized the evolved POIs by cloning the mutated POI genes into
804 a backbone for single-copy integration. A W303 strain was transformed with these plasmids as
805 well as plasmids for single-copy integration of constructs in which the transcription of a
806 fluorescent protein was driven by *LIP* (in case of El222) or *tetOpr* (PEST-rtTA). Integration of single
807 copies was confirmed by PCR in all transformants. For measuring the transcriptional rate of PhyB-
808 Pif3 as a split Gal4 system, we used the strain from ref.[110]

809 Light conditions

810 Throughout, we handled cells sensitive to blue light under red light and red-responsive cells as
811 well as PCB under green light. Plates were otherwise always wrapped in aluminum foil.

812 For administering blue light to induce El222, we used commercial blue light LED panels (HQRP,
813 USA). The panels were placed inside incubators at a distance of 20 cm above the agar plates or a
814 spinning wheel of liquid cell culture tubes. For evolving color-shifted El222 variants, we used LEDs
815 with peaks around green (525 nm), yellow (575 nm), orange (615 nm), and red (660 nm) (Mouser,
816 Switzerland). For characterizing color-shifted El222 variants, we used 488 nm (JDSU, China), 514
817 nm (Oxxius, France), 561 nm (CrystaLaser, USA), and 641 nm (Coherent, USA) lasers. For inducing
818 optogenetics during microscopy, we used diascopic light and placed a green interference filter in
819 the optical path (Nikon, Switzerland) when needed. For administering red and far-red light that
820 switches PhyB-Pif3, we used red light panels (Amats, China) with a peak around 650 nm and
821 custom-made printed circuit boards with 750 nm far-red LEDs (Roithner Lasertechnik, Austria).

822 The spectral characteristics of the light sources, measured using an ST-VIS-25 spectrometer (Ocean
823 Insight, USA) are shown in Supplementary Fig. 1.

824 To control the LEDs or lasers, we used an NI USB 6501 (Texas Instruments, USA) I/O device. The
825 system was run using a custom Matlab script (**Code availability**). The regime of pulsing light could
826 be adjusted with a precision of less than one second.

827 Quantification of the transition from *cln1-3Δ* arrest with optogenetic cell-cycle
828 control

829 To score the portion of cells that bud in response to a pulse of light (Fig. 2 B), we tested *cln1-3Δ*
830 *MET3pr-CLN2* and *cln1-3Δ clb3-6Δ pRD-TW1* cells with additional *EL222* and LIP-controlled Cdk1
831 cyclins, as indicated. After loading cells into a microfluidic chip and growing them for 4-5 hrs, we
832 supplied methionine, which shuts off *MET3pr*. Two hours after methionine had been added, cells
833 were large and unbudded (G1 arrest). Different optogenetic constructs (*LIP-CLB5* and *LIP-CLN2*)
834 were activated by using diascopic light from the microscope set to 80% of maximal intensity for 20
835 min or 40 min, depending on the experiment. Cells were imaged every 10 min.

836 ## Optovolution experiments on agar plates

837 Prior to evolution, cells were propagated under the light pulsing regime that allowed proliferation
838 on SCD agar plates until growth saturation. To increase the mutational diversity of the population,
839 cells were then mutagenized by exposing them for 10 sec to UV light with 254 nm emission peak
840 (model G30T8, Sankyo Denki, Japan). We scraped cells from one plate and resuspended them in 1
841 mL of liquid SCD medium prewarmed to 30°C. Then, we plated 100-200 µL of cell culture on fresh
842 agar plates and chose the desired selection pressure by adjusting the light pulse regime. After
843 three days of growth, we replica-plated the cells to provide fresh nutrients. After another two days
844 of growth, we picked isolated colonies by restreaking them on fresh SCD plates, and allowed them
845 to grow for another two days. Finally, we identified the mutations by Sanger sequencing the POI
846 gene. The whole process took about seven days per screen.

847 ## Long-term continuous optovolution in liquid medium

848 As in the agar plate experiments, cells were propagated on SCD plates and UV-mutagenized. We
849 scraped cells from one plate and resuspended them in 1 mL of liquid SCD medium. We added 200
850 µL from this suspension to 100 mL of liquid SCD medium. We used transparent 250 mL Erlenmeyer
851 flasks (VWR, Switzerland). Cell cultures were grown in an incubator shaker (Infors HT, Switzerland)
852 set at 250 rotations per minute and 30°C. For administering pulsing light, we used panels of blue
853 LEDs mounted on a custom rack inside the incubator.

854 To prevent the cultures from reaching saturation, we diluted them in warm SCD medium to a final
855 OD (660 nm) of 0.04 every 12 hrs. We performed the experiment for a week, after which we
856 proceeded to Sanger sequencing bulk culture genomic DNA for the POI gene.

857 ## Mutation identification

858 To screen for mutations in the genes of interest, we performed Sanger sequencing (Microsynth
859 AG, Switzerland) using primers that span the coding sequence of interest. The identified mutations
860 were confirmed by sequencing the plasmids after cloning the POI gene.

861 For identifying mutations in the genome, we performed paired-end whole genome sequencing of
862 the evolved and ancestral genomes. The sequencing was performed using 150 bp long reads on
863 the DNBseq platform with a total data output of 1 Gb. The ancestral and the evolved reads were
864 then mapped onto the W303 reference genome using Bowtie 2. For variant calling, we used
865 BCFtools. The mutations were called if they appeared in the evolved but not the ancestral
866 genome, and if they were sequenced with a depth of at least 10.

867 ## Variant characterization

868 In all cases, strains were grown to saturation for 18-20 h, diluted, and then allowed to reach log
869 phase. Transcriptional activities were scaled to the maxGAL1 unit, where 1 maxGAL1 corresponds

870 to the steady-state expression of *GAL1pr* in synthetic complete medium containing 3% raffinose
871 (w/v) and 2% galactose (w/v)[88].

872 For characterizing the light-sensitized and color-shifted El222 variants, we cloned mutant *EL222*
873 into plasmids that inserted as single copies into the budding yeast genome, and transformed a
874 strain that contained a single-copy *LIP-ymScarletI* reporter with the plasmids. While *LIP-ymScarletI*
875 was the reporter of choice for characterizing light-sensitized variants to avoid excitation light
876 inducing the mutant El222, it has a comparatively lower sensitivity than a *yEVenus* reporter.
877 Hence, for carefully characterizing the leakiness of wt-El222 and low-leakiness variants, we
878 introduced them into a strain containing a single-copy *LIP-yEVenus* reporter. All variants were
879 induced in log phase in liquid culture for 6 h. The light-sensitized or low-leakiness variants were
880 tested under two different light pulse regimes, high or low time-averaged LED intensity (Fig. 4 B, F,
881 J). The low LED regime corresponds to the blue LEDs (Supplementary Fig. 1) pulsed for 10 sec
882 every 5 min. The high LED regime corresponds to 30 sec on, 30 sec off every minute. The color-
883 shifted variants were induced under the presence of laser light of different wavelengths
884 (Supplementary Fig. 1). For characterizing the dynamics of the evolved variants with timelapse
885 fluorescence microscopy, we used variants of the reporters in which the corresponding
886 fluorescent proteins are fused to the PEST degron, reducing the half-life of the reporters. From the
887 measured fluorescence values, we subtracted the fluorescence levels of cells containing only the
888 corresponding *LIP*-based reporter, which showed elevated fluorescence levels compared to wild-
889 type (no-reporter) cells (Supplementary Fig. 2).

890 For characterizing the effect of *yor1Δ* in combination with the PhyB-Pif3 system, we used a strain
891 from ref. [110] with a *GAL1pr-Venus* reporter. In case PCB was used, cells were incubated with it in
892 darkness for 1 hr before exposure to red light. We used 30 sec on, 30 sec off red light with an
893 emission peak around 650 nm delivered for 6 h to cells grown in SCD liquid medium tubes on a
894 spinning wheel. After that, the level of expression was measured using fluorescence microscopy.
895 Previous measurements of *GAL1pr* activity in glucose showed that it does not exhibit leakiness
896 that is distinguishable from wild-type cells without a reporter[88]. Hence, from the measured values,
897 we subtracted the background fluorescence of a wild-type strain. To convert the expression levels
898 to maxGAL1 units, we measured the steady-state expression level of *GAL1pr-Venus* in the same
899 strain by growing it in SC medium with 3% raffinose (w/v) and 2% galactose medium (w/v).

900 For quantifying the activity of PEST-rtTA mutants, we introduced them into strains with a *tetOpr-*
901 *yEVenus-PEST* reporter. We grew the strains with or without doxycycline for 6 hrs and then imaged
902 them by fluorescence microscopy. From the measured values, we subtracted the corresponding
903 background fluorescence values of the strain containing only a *tetOpr-yEVenus-PEST* reporter in
904 the corresponding medium.

905 ### Microscopy and image analysis

906 Images were recorded using a Nikon Ti2-E (Nikon, Switzerland) microscope equipped with a 60x
907 oil, N.A. 1.40 objective and a Hamamatsu Orca-Flash 4.0 camera (Hamamatsu, Japan). The
908 microscope was controlled using NIS-Elements software and the Nikon Perfect Focus System.
909 When performing timelapse microscopy to monitor the dynamic properties of El222, we induced
910 with diascopic light, as described previously. To not induce El222 while observing cells under the
911 microscope, we used a band-pass green interference filter (Nikon, Switzerland) placed between
912 the diascopic light and the sample. The characteristics of this light are presented in Supplementary
913 Fig. 1. The diascopic light was set to either 80% of maximal intensity, when inducing low-leakiness
914 variants (Fig. 4 G), to 20% of maximal intensity when inducing light-sensitized variants (Fig. 4 C), or
915 to 80% of maximal intensity with a green interference filter when inducing color-shifted variants
916 (Fig. 4 K). Image analysis was performed using YeaZ[141], a deep neural network for analyzing images
917 of yeast cells.

918 Statistics and reproducibility

919 No statistical method was used to predetermine sample size. The values in the heatmaps in Figs. 4
920 and 6 are rounded based on the first significant digit of the standard error of the mean.

921 Data and material availability

922 The characteristics of the systems measured in this study have been added to the Inducible
923 Transcriptional Systems Database (https://promoter-benchmark.epfl.ch/)[88]. Any additional data
924 that support the findings of this study are available from the corresponding author upon request.

925 Code availability

926 The Matlab code for controlling the light pulses is available at:

927 https://github.com/rahi-lab/optogenetic_controller_script/.

928 # References

929 1. Mills, D. R., Peterson, R. L. & Spiegelman, S. An extracellular Darwinian experiment with a self-
930 duplicating nucleic acid molecule. *Proc. Natl. Acad. Sci. U.S.A.* **58**, 217–224 (1967).
931 2. Kuchner, O. & Arnold, F. H. Directed evolution of enzyme catalysts. *Trends in Biotechnology* **15**,
932 523–530 (1997).
933 3. Schmidt-Dannert, C. & Arnold, F. H. Directed evolution of industrial enzymes. *Trends in*
934 *Biotechnology* **17**, 135–136 (1999).
935 4. Packer, M. S. & Liu, D. R. Methods for the directed evolution of proteins. *Nat Rev Genet* **16**,
936 379–394 (2015).
937 5. Wang, Y. *et al.* Directed Evolution: Methodologies and Applications. *Chem. Rev.* **121**, 12384–
938 12444 (2021).
939 6. Crameri, A., Whitehorn, E. A., Tate, E. & Stemmer, W. P. C. Improved Green Fluorescent
940 Protein by Molecular Evolution Using DNA Shuffling. *Nat Biotechnol* **14**, 315–319 (1996).
941 7. Campbell, R. E. *et al.* A monomeric red fluorescent protein. *Proc. Natl. Acad. Sci. U.S.A.* **99**,
942 7877–7882 (2002).
943 8. Li, Y. *et al.* Directed evolution of human T-cell receptors with picomolar affinities by phage
944 display. *Nat Biotechnol* **23**, 349–354 (2005).
945 9. Xu, L. *et al.* Directed Evolution of High-Affinity Antibody Mimics Using mRNA Display.
946 *Chemistry & Biology* **9**, 933–942 (2002).
947 10. Ravikumar, A., Arzumanyan, G. A., Obadi, M. K. A., Javanpour, A. A. & Liu, C. C. Scalable,
948 Continuous Evolution of Genes at Mutation Rates above Genomic Error Thresholds. *Cell* **175**,
949 1946-1957.e13 (2018).
950 11. Yi, X., Khey, J., Kazlauskas, R. J. & Travisano, M. Plasmid hypermutation using a targeted
951 artificial DNA replisome. *Sci. Adv.* **7**, eabg8712 (2021).

952 12. Moore, C. L., Papa, L. J. & Shoulders, M. D. A Processive Protein Chimera Introduces Mutations
953 across Defined DNA Regions *In Vivo*. *J. Am. Chem. Soc.* **140**, 11560–11564 (2018).
954 13. Arnold, F. H. Design by Directed Evolution. *Acc. Chem. Res.* **31**, 125–131 (1998).
955 14. Esvelt, K. M., Carlson, J. C. & Liu, D. R. A system for the continuous directed evolution of
956 biomolecules. *Nature* **472**, 499–503 (2011).
957 15. Badran, A. H. & Liu, D. R. In vivo continuous directed evolution. *Current Opinion in Chemical*
958 *Biology* **24**, 1–10 (2015).
959 16. Molina, R. S. *et al.* In vivo hypermutation and continuous evolution. *Nat Rev Methods Primers*
960 **2**, 36 (2022).
961 17. Crook, N. *et al.* In vivo continuous evolution of genes and pathways in yeast. *Nat Commun* **7**,
962 13051 (2016).
963 18. Morrison, M. S., Podracky, C. J. & Liu, D. R. The developing toolkit of continuous directed
964 evolution. *Nat Chem Biol* **16**, 610–619 (2020).
965 19. Hubbard, B. P. *et al.* Continuous directed evolution of DNA-binding proteins to improve TALEN
966 specificity. *Nat Methods* **12**, 939–942 (2015).
967 20. Pu, J., Zinkus-Boltz, J. & Dickinson, B. C. Evolution of a split RNA polymerase as a versatile
968 biosensor platform. *Nat Chem Biol* **13**, 432–438 (2017).
969 21. Xie, V. C., Pu, J., Metzger, B. P., Thornton, J. W. & Dickinson, B. C. Contingency and chance
970 erase necessity in the experimental evolution of ancestral proteins. *eLife* **10**, e67336 (2021).
971 22. Doyon, J. B., Pattanayak, V., Meyer, C. B. & Liu, D. R. Directed Evolution and Substrate
972 Specificity Profile of Homing Endonuclease I-SceI. *J. Am. Chem. Soc.* **128**, 2477–2484 (2006).
973 23. Kleinstiver, B. P. *et al.* Engineered CRISPR-Cas9 nucleases with altered PAM specificities.
974 *Nature* **523**, 481–485 (2015).
975 24. Lee, J. K. *et al.* Directed evolution of CRISPR-Cas9 to increase its specificity. *Nat Commun* **9**,
976 3048 (2018).

977 25. Spisak, S., O'Brien, B. & Ostermeier, M. A bacterial dual positive and negative selection system
978 for dCas9 activity. *PLoS ONE* **17**, e0269270 (2022).
979 26. Goldberg, G. W. *et al.* Engineered dual selection for directed evolution of SpCas9 PAM
980 specificity. *Nat Commun* **12**, 349 (2021).
981 27. Casini, A. *et al.* A highly specific SpCas9 variant is identified by in vivo screening in yeast. *Nat*
982 *Biotechnol* **36**, 265–271 (2018).
983 28. Sadeghi, A., Dervey, R., Gligorovski, V., Labagnara, M. & Rahi, S. J. The optimal strategy
984 balancing risk and speed predicts DNA damage checkpoint override times. *Nat. Phys.* (2022)
985 doi:10.1038/s41567-022-01601-3.
986 29. Chen, Z. *et al.* De novo design of protein logic gates. *Science* **368**, 78–84 (2020).
987 30. Gao, X. J., Chong, L. S., Kim, M. S. & Elowitz, M. B. Programmable protein circuits in living cells.
988 *Science* **361**, 1252–1258 (2018).
989 31. Fink, T. *et al.* Design of fast proteolysis-based signaling and logic circuits in mammalian cells.
990 *Nat Chem Biol* **15**, 115–122 (2019).
991 32. Omersa, N., Aden, S., Kisovec, M., Podobnik, M. & Anderluh, G. Design of Protein Logic Gate
992 System Operating on Lipid Membranes. *ACS Synth. Biol.* **9**, 316–328 (2020).
993 33. Vishweshwaraiah, Y. L., Chen, J., Chirasani, V. R., Tabdanov, E. D. & Dokholyan, N. V. Two-input
994 protein logic gate for computation in living cells. *Nat Commun* **12**, 6615 (2021).
995 34. Berman, C. M. *et al.* An Adaptable Platform for Directed Evolution in Human Cells. *J. Am.*
996 *Chem. Soc.* **140**, 18093–18103 (2018).
997 35. English, J. G. *et al.* VEGAS as a Platform for Facile Directed Evolution in Mammalian Cells. *Cell*
998 **178**, 748-761.e17 (2019).
999 36. Groseclose, T. M., Rondon, R. E., Herde, Z. D., Aldrete, C. A. & Wilson, C. J. Engineered systems
1000 of inducible anti-repressors for the next generation of biological programming. *Nat Commun*
1001 **11**, 4440 (2020).

1002 37. Sanchez, M. I. & Ting, A. Y. Directed evolution improves the catalytic efficiency of TEV
1003 protease. *Nat Methods* **17**, 167–174 (2020).
1004 38. Tominaga, M., Nozaki, K., Umeno, D., Ishii, J. & Kondo, A. Robust and flexible platform for
1005 directed evolution of yeast genetic switches. *Nat Commun* **12**, 1846 (2021).
1006 39. Klauser, B., Atanasov, J., Siewert, L. K. & Hartig, J. S. Ribozyme-Based Aminoglycoside Switches
1007 of Gene Expression Engineered by Genetic Selection in *S. cerevisiae*. *ACS Synth. Biol.* **4**, 516–
1008 525 (2015).
1009 40. Skjoedt, M. L. *et al.* Engineering prokaryotic transcriptional activators as metabolite biosensors
1010 in yeast. *Nat Chem Biol* **12**, 951–958 (2016).
1011 41. Snoek, T. *et al.* Evolution-guided engineering of small-molecule biosensors. *Nucleic Acids*
1012 *Research* **48**, e3–e3 (2020).
1013 42. Usherenko, S. *et al.* Photo-sensitive degron variants for tuning protein stability by light. *BMC*
1014 *Syst Biol* **8**, 128 (2014).
1015 43. Lu, H. *et al.* A Yeast System for Discovering Optogenetic Inhibitors of Eukaryotic Translation
1016 Initiation. *ACS Synth. Biol.* **8**, 744–757 (2019).
1017 44. Wang, W. *et al.* A light- and calcium-gated transcription factor for imaging and manipulating
1018 activated neurons. *Nat Biotechnol* **35**, 864–871 (2017).
1019 45. Woloschuk, R. M., Reed, P. M. M., McDonald, S., Uppalapati, M. & Woolley, G. A. Yeast Two-
1020 Hybrid Screening of Photoswitchable Protein–Protein Interaction Libraries. *Journal of*
1021 *Molecular Biology* **432**, 3113–3126 (2020).
1022 46. Taslimi, A. *et al.* Optimized second-generation CRY2–CIB dimerizers and photoactivatable Cre
1023 recombinase. *Nat Chem Biol* **12**, 425–430 (2016).
1024 47. Huang, Z. *et al.* Creating Red Light-Switchable Protein Dimerization Systems as Genetically
1025 Encoded Actuators with High Specificity. *ACS Synth. Biol.* **9**, 3322–3333 (2020).

1026 48. Guntas, G. *et al.* Engineering an improved light-induced dimer (iLID) for controlling the
1027 localization and activity of signaling proteins. *Proc. Natl. Acad. Sci. U.S.A.* **112**, 112–117 (2015).
1028 49. Reis, J. M. *et al.* Discovering Selective Binders for Photoswitchable Proteins Using Phage
1029 Display. *ACS Synth. Biol.* **7**, 2355–2364 (2018).
1030 50. Wang, H. *et al.* LOVTRAP: an optogenetic system for photoinduced protein dissociation. *Nat*
1031 *Methods* **13**, 755–758 (2016).
1032 51. Kawano, F., Aono, Y., Suzuki, H. & Sato, M. Fluorescence Imaging-Based High-Throughput
1033 Screening of Fast- and Slow-Cycling LOV Proteins. *PLoS ONE* **8**, e82693 (2013).
1034 52. Yokobayashi, Y., Weiss, R. & Arnold, F. H. Directed evolution of a genetic circuit. *Proc. Natl.*
1035 *Acad. Sci. U.S.A.* **99**, 16587–16591 (2002).
1036 53. Maranhao, A. C. & Ellington, A. D. Evolving Orthogonal Suppressor tRNAs To Incorporate
1037 Modified Amino Acids. *ACS Synth. Biol.* **6**, 108–119 (2017).
1038 54. Baumschlager, A., Weber, Y., Cánovas, D., Dionisi, S. & Khammash, M. *Enhancing the*
1039 *Performance of Magnets Photosensors through Directed Evolution*.
1040 http://biorxiv.org/lookup/doi/10.1101/2022.11.14.516313 (2022)
1041 doi:10.1101/2022.11.14.516313.
1042 55. Meyer, A. J., Segall-Shapiro, T. H., Glassey, E., Zhang, J. & Voigt, C. A. Escherichia coli
1043 "Marionette" strains with 12 highly optimized small-molecule sensors. *Nat Chem Biol* **15**, 196–
1044 204 (2019).
1045 56. Tashiro, Y., Fukutomi, H., Terakubo, K., Saito, K. & Umeno, D. A nucleoside kinase as a dual
1046 selector for genetic switches and circuits. *Nucleic Acids Research* **39**, e12–e12 (2011).
1047 57. Taylor, N. D. *et al.* Engineering an allosteric transcription factor to respond to new ligands. *Nat*
1048 *Methods* **13**, 177–183 (2016).
1049 58. Tang, S.-Y., Fazelinia, H. & Cirino, P. C. AraC Regulatory Protein Mutants with Altered Effector
1050 Specificity. *J. Am. Chem. Soc.* **130**, 5267–5271 (2008).

1051 59. Lee, S. K. *et al.* Directed Evolution of AraC for Improved Compatibility of Arabinose- and
1052 Lactose-Inducible Promoters. *Appl Environ Microbiol* **73**, 5711–5715 (2007).
1053 60. Shong, J., Huang, Y.-M., Bystroff, C. & Collins, C. H. Directed Evolution of the Quorum-Sensing
1054 Regulator EsaR for Increased Signal Sensitivity. *ACS Chem. Biol.* **8**, 789–795 (2013).
1055 61. Nomura, Y. & Yokobayashi, Y. Dual selection of a genetic switch by a single selection marker.
1056 *Biosystems* **90**, 115–120 (2007).
1057 62. Muranaka, N., Sharma, V., Nomura, Y. & Yokobayashi, Y. An efficient platform for genetic
1058 selection and screening of gene switches in Escherichia coli. *Nucleic Acids Research* **37**, e39–
1059 e39 (2009).
1060 63. Sharma, V., Nomura, Y. & Yokobayashi, Y. Engineering Complex Riboswitch Regulation by Dual
1061 Genetic Selection. *J. Am. Chem. Soc.* **130**, 16310–16315 (2008).
1062 64. Richter, F. *et al.* Engineering of temperature- and light-switchable Cas9 variants. *Nucleic Acids*
1063 *Research* **44**, gkw930 (2013).
1064 65. Tominaga, M., Ike, K., Kawai-Noma, S., Saito, K. & Umeno, D. Rapid and Liquid-Based Selection
1065 of Genetic Switches Using Nucleoside Kinase Fused with Aminoglycoside Phosphotransferase.
1066 *PLoS ONE* **10**, e0120243 (2015).
1067 66. Saeki, K., Tominaga, M., Kawai-Noma, S., Saito, K. & Umeno, D. Rapid Diversification of BetI-
1068 Based Transcriptional Switches for the Control of Biosynthetic Pathways and Genetic Circuits.
1069 *ACS Synth. Biol.* **5**, 1201–1210 (2016).
1070 67. Ike, K. *et al.* Evolutionary Design of Choline-Inducible and -Repressible T7-Based Induction
1071 Systems. *ACS Synth. Biol.* **4**, 1352–1360 (2015).
1072 68. Guntas, G., Mansell, T. J., Kim, J. R. & Ostermeier, M. Directed evolution of protein switches
1073 and their application to the creation of ligand-binding proteins. *Proc. Natl. Acad. Sci. U.S.A.*
1074 **102**, 11224–11229 (2005).

1075 69. Tashiro, Y. *et al.* Directed evolution of the autoinducer selectivity of *Vibrio fischeri* LuxR. *J. Gen.*
1076 *Appl. Microbiol.* **62**, 240–247 (2016).
1077 70. Ellefson, J. W., Ledbetter, M. P. & Ellington, A. D. Directed evolution of a synthetic phylogeny
1078 of programmable Trp repressors. *Nat Chem Biol* **14**, 361–367 (2018).
1079 71. Boeke, J. D., Trueheart, J., Natsoulis, G. & Fink, G. R. [10] 5-Fluoroorotic acid as a selective
1080 agent in yeast molecular genetics. in *Methods in Enzymology* vol. 154 164–175 (Elsevier,
1081 1987).
1082 72. Tague, N., Coriano-Ortiz, C., Sheets, M. B. & Dunlop, M. J. *Light Inducible Protein Degradation*
1083 *in E. Coli with the LOVdeg Tag*. https://elifesciences.org/reviewed-preprints/87303v2 (2024)
1084 doi:10.7554/eLife.87303.2.
1085 73. Nguyen, N. T., Liu, S., Han, G., Zhou, Y. & Huang, K. Nano-optogenetic CAR-T Cell
1086 Immunotherapy. in *Cancer Immunotherapy* (eds. Siciliano, V. & Ceroni, F.) vol. 2748 267–278
1087 (Springer US, New York, NY, 2024).
1088 74. Song, G. *et al.* Rapid characterization of anti-CRISPR proteins and optogenetically engineered
1089 variants using a versatile plasmid interference system. *Nucleic Acids Research* **51**, 12381–
1090 12396 (2023).
1091 75. Levskaya, A., Weiner, O. D., Lim, W. A. & Voigt, C. A. Spatiotemporal control of cell signalling
1092 using a light-switchable protein interaction. *Nature* **461**, 997–1001 (2009).
1093 76. Cui, M. *et al.* A single-component, light-assisted uncaging switch for endoproteolytic release.
1094 *Nat Chem Biol* (2023) doi:10.1038/s41589-023-01480-6.
1095 77. Nzigou Mombo, B. *et al.* Reversible photoregulation of cell-cell adhesions with opto-E-
1096 cadherin. *Nat Commun* **14**, 6292 (2023).
1097 78. Legnini, I. *et al.* Spatiotemporal, optogenetic control of gene expression in organoids. *Nat*
1098 *Methods* **20**, 1544–1552 (2023).

1099 79. Ho, E. K. *et al.* Dynamics of an incoherent feedforward loop drive ERK-dependent pattern
1100 formation in the early *Drosophila* embryo. *Development* **150**, dev201818 (2023).
1101 80. Pal, A. A. *et al.* Optogenetic clustering and membrane translocation of the BcLOV4
1102 photoreceptor. *Proc. Natl. Acad. Sci. U.S.A.* **120**, e2221615120 (2023).
1103 81. Mahlandt, E. K. *et al.* Opto-RhoGEFs, an optimized optogenetic toolbox to reversibly control
1104 Rho GTPase activity on a global to subcellular scale, enabling precise control over vascular
1105 endothelial barrier strength. *eLife* **12**, RP84364 (2023).
1106 82. Lim, C. K., Yeoh, J. W., Kunartama, A. A., Yew, W. S. & Poh, C. L. A biological camera that
1107 captures and stores images directly into DNA. *Nat Commun* **14**, 3921 (2023).
1108 83. Elsaid, R., Mikdache, A., Diabangouaya, P., Gros, G. & Hernández, P. P. *A Non-Invasive*
1109 *Photoactivatable Split-Cre Recombinase System for Genome Engineering in Zebrafish*.
1110 http://biorxiv.org/lookup/doi/10.1101/2023.06.23.546268 (2023)
1111 doi:10.1101/2023.06.23.546268.
1112 84. De Belly, H. *et al.* Cell protrusions and contractions generate long-range membrane tension
1113 propagation. *Cell* **186**, 3049-3061.e15 (2023).
1114 85. Benisch, M., Benzinger, D., Kumar, S., Hu, H. & Khammash, M. Optogenetic closed-loop
1115 feedback control of the unfolded protein response optimizes protein production. *Metabolic*
1116 *Engineering* **77**, 32–40 (2023).
1117 86. Sheets, M. B., Tague, N. & Dunlop, M. J. An optogenetic toolkit for light-inducible antibiotic
1118 resistance. *Nat Commun* **14**, 1034 (2023).
1119 87. Zoltowski, B. D., Vaccaro, B. & Crane, B. R. Mechanism-based tuning of a LOV domain
1120 photoreceptor. *Nat Chem Biol* **5**, 827–834 (2009).
1121 88. Gligorovski, V., Sadeghi, A. & Rahi, S. J. Multidimensional characterization of inducible
1122 promoters and a highly light-sensitive LOV-transcription factor. *Nat Commun* **14**, 3810 (2023).

1123 89. Pudasaini, A., El-Arab, K. K. & Zoltowski, B. D. LOV-based optogenetic devices: light-driven
1124 modules to impart photoregulated control of cellular signaling. *Front. Mol. Biosci.* **2**, (2015).
1125 90. Adir, O. *et al.* Synthetic cells with self-activating optogenetic proteins communicate with
1126 natural cells. *Nat Commun* **13**, 2328 (2022).
1127 91. Pan, H. *et al.* Engineered NIR light-responsive bacteria as anti-tumor agent for targeted and
1128 precise cancer therapy. *Chemical Engineering Journal* **426**, 130842 (2021).
1129 92. Wang, Z., Yan, Y. & Zhang, H. Design and Characterization of an Optogenetic System in *Pichia*
1130 *pastoris*. *ACS Synth. Biol.* **11**, 297–307 (2022).
1131 93. Zhao, E. M. *et al.* Optogenetic regulation of engineered cellular metabolism for microbial
1132 chemical production. *Nature* **555**, 683–687 (2018).
1133 94. Motta-Mena, L. B. *et al.* An optogenetic gene expression system with rapid activation and
1134 deactivation kinetics. *Nat Chem Biol* **10**, 196–202 (2014).
1135 95. Baaske, J. *et al.* Dual-controlled optogenetic system for the rapid down-regulation of protein
1136 levels in mammalian cells. *Sci Rep* **8**, 15024 (2018).
1137 96. LaBelle, J. *et al.* TAEL 2.0: An Improved Optogenetic Expression System for Zebrafish. *Zebrafish*
1138 **18**, 20–28 (2021).
1139 97. Molin, M. *et al.* Protein kinase A controls yeast growth in visible light. *BMC Biol* **18**, 168 (2020).
1140 98. Barolet, D. Light-Emitting Diodes (LEDs) in Dermatology. *Seminars in Cutaneous Medicine and*
1141 *Surgery* **27**, 227–238 (2008).
1142 99. Akagi, H., Shimizu, H. & Toya, Y. Multicolor optogenetics for regulating flux ratio of three
1143 glycolytic pathways using EL222 and CcaSR in *Escherichia coli*. *Biotech & Bioengineering*
1144 bit.28628 (2023) doi:10.1002/bit.28628.
1145 100. Kramer, M. M., Mühlhäuser, W. W. D., Weber, W. & Radziwill, G. Multichromatic Control of
1146 Signaling Pathways in Mammalian Cells. *Advanced Biology* **5**, 2000196 (2021).

1147 101. Ochoa-Fernandez, R. *et al.* Optogenetic control of gene expression in plants in the
1148 presence of ambient white light. *Nat Methods* **17**, 717–725 (2020).
1149 102. Redchuk, T. A. *et al.* Optogenetic regulation of endogenous proteins. *Nat Commun* **11**, 605
1150 (2020).
1151 103. Losi, A., Gardner, K. H. & Möglich, A. Blue-Light Receptors for Optogenetics. *Chem. Rev.*
1152 **118**, 10659–10709 (2018).
1153 104. Remeeva, A. *et al.* Insights into the mechanisms of light-oxygen-voltage domain color
1154 tuning from a set of high-resolution X-ray structures. *Proteins* **89**, 1005–1016 (2021).
1155 105. Nikolaev, A. *et al.* Fine spectral tuning of a flavin-binding fluorescent protein for multicolor
1156 imaging. *Journal of Biological Chemistry* **299**, 102977 (2023).
1157 106. Toettcher, J. E., Gong, D., Lim, W. A. & Weiner, O. D. Light-based feedback for controlling
1158 intracellular signaling dynamics. *Nat Methods* **8**, 837–839 (2011).
1159 107. Yang, X., Jost, A. P.-T., Weiner, O. D. & Tang, C. A light-inducible organelle-targeting system
1160 for dynamically activating and inactivating signaling in budding yeast. *MBoC* **24**, 2419–2430
1161 (2013).
1162 108. Shimizu-Sato, S., Huq, E., Tepperman, J. M. & Quail, P. H. A light-switchable gene promoter
1163 system. *Nat Biotechnol* **20**, 1041–1044 (2002).
1164 109. Pathak, G. P., Strickland, D., Vrana, J. D. & Tucker, C. L. Benchmarking of optical dimerizer
1165 systems. *ACS Synth. Biol.* **3**, 832–838 (2014).
1166 110. Milias-Argeitis, A. *et al. In silico* feedback for in vivo regulation of a gene expression circuit.
1167 *Nat Biotechnol* **29**, 1114–1116 (2011).
1168 111. Oda, S., Sato-Ebine, E., Nakamura, A., Kimura, K. D. & Aoki, K. *Optogenetic Control of Cell*
1169 *Signaling with Red/Far-Red Light-Responsive Optogenetic Tools in* Caenorhabditis Elegans.
1170 http://biorxiv.org/lookup/doi/10.1101/2022.08.12.503710 (2022)
1171 doi:10.1101/2022.08.12.503710.

1172 112. Uda, Y. *et al.* Efficient synthesis of phycocyanobilin in mammalian cells for optogenetic
1173 control of cell signaling. *Proc. Natl. Acad. Sci. U.S.A.* **114**, 11962–11967 (2017).
1174 113. Müller, K. *et al.* Synthesis of phycocyanobilin in mammalian cells. *Chem. Commun.* **49**, 8970
1175 (2013).
1176 114. Hochrein, L., Machens, F., Messerschmidt, K. & Mueller-Roeber, B. PhiReX: a
1177 programmable and red light-regulated protein expression switch for yeast. *Nucleic Acids*
1178 *Research* **45**, 9193–9205 (2017).
1179 115. Gossen, M. *et al.* Transcriptional Activation by Tetracyclines in Mammalian Cells. *Science*
1180 **268**, 1766–1769 (1995).
1181 116. Mateus, C. & Avery, S. V. Destabilized green fluorescent protein for monitoring dynamic
1182 changes in yeast gene expression with flow cytometry. *Yeast* **16**, 1313–1323 (2000).
1183 117. Leopold, A. V., Chernov, K. G. & Verkhusha, V. V. Optogenetically controlled protein kinases
1184 for regulation of cellular signaling. *Chem. Soc. Rev.* **47**, 2454–2484 (2018).
1185 118. de Mena, L., Rizk, P. & Rincon-Limas, D. E. Bringing light to transcription: the optogenetics
1186 repertoire. *Front. Genet.* **9**, 518 (2018).
1187 119. Niopek, D. *et al.* Engineering light-inducible nuclear localization signals for precise
1188 spatiotemporal control of protein dynamics in living cells. *Nat Commun* **5**, 4404 (2014).
1189 120. Renicke, C., Schuster, D., Usherenko, S., Essen, L.-O. & Taxis, C. A LOV2 Domain-Based
1190 Optogenetic Tool to Control Protein Degradation and Cellular Function. *Chemistry & Biology*
1191 **20**, 619–626 (2013).
1192 121. Dagliyan, O. *et al.* Engineering extrinsic disorder to control protein activity in living cells.
1193 *Science* **354**, 1441–1444 (2016).
1194 122. Chen, J., Vishweshwaraiah, Y. L., Mailman, R. B., Tabdanov, E. D. & Dokholyan, N. V. A
1195 noncommutative combinatorial protein logic circuit controls cell orientation in
1196 nanoenvironments. *Sci. Adv.* **9**, eadg1062 (2023).

1197 123. Nihongaki, Y., Kawano, F., Nakajima, T. & Sato, M. Photoactivatable CRISPR-Cas9 for
1198 optogenetic genome editing. *Nat Biotechnol* **33**, 755–760 (2015).
1199 124. Mathony, J., Aschenbrenner, S., Becker, P. & Niopek, D. Dissecting the Determinants of
1200 Domain Insertion Tolerance and Allostery in Proteins. *Advanced Science* **10**, 2303496 (2023).
1201 125. Weinberg, B. H. *et al.* High-performance chemical- and light-inducible recombinases in
1202 mammalian cells and mice. *Nat Commun* **10**, 4845 (2019).
1203 126. Dagliyan, O. *et al.* Computational design of chemogenetic and optogenetic split proteins.
1204 *Nat Commun* **9**, 4042 (2018).
1205 127. Rahi, S. J., Pecani, K., Ondracka, A., Oikonomou, C. & Cross, F. R. The CDK-APC/C oscillator
1206 predominantly entrains periodic cell-cycle transcription. *Cell* **165**, 475–487 (2016).
1207 128. Richardson, H., Lew, D. J., Henze, M., Sugimoto, K. & Reed, S. I. Cyclin-B homologs in
1208 Saccharomyces cerevisiae function in S phase and in G2. *Genes Dev.* **6**, 2021–2034 (1992).
1209 129. Rahi, S. J. *et al.* Oscillatory stimuli differentiate adapting circuit topologies. *Nat Methods*
1210 **14**, 1010–1016 (2017).
1211 130. Loog, M. & Morgan, D. O. Cyclin specificity in the phosphorylation of cyclin-dependent
1212 kinase substrates. *Nature* **434**, 104–108 (2005).
1213 131. Morgan, D. O. *The Cell Cycle: Principles of Control*. (Published by New Science Press in
1214 association with Oxford University Press; Distributed inside North America by Sinauer
1215 Associates, Publishers, London: Sunderland, MA, 2007).
1216 132. Levine, K., Kiang, L., Jacobson, M. D., Fisher, R. P. & Cross, F. R. Directed Evolution to
1217 Bypass Cyclin Requirements for the Cdc28p Cyclin-Dependent Kinase. *Molecular Cell* **4**, 353–
1218 363 (1999).
1219 133. Tyers, M. The cyclin-dependent kinase inhibitor p40SIC1 imposes the requirement for Cln
1220 G1 cyclin function at Start. *Proc. Natl. Acad. Sci. U.S.A.* **93**, 7772–7776 (1996).

1221 134. Jin, Y. H. *et al.* The Multiple Biological Roles of the 3′→5′ Exonuclease of *Saccharomyces*
1222 *cerevisiae* DNA Polymerase δ Require Switching between the Polymerase and Exonuclease
1223 Domains. *Molecular and Cellular Biology* **25**, 461–471 (2005).
1224 135. Lang, G. I. & Murray, A. W. Estimating the Per-Base-Pair Mutation Rate in the Yeast
1225 *Saccharomyces cerevisiae*. *Genetics* **178**, 67–82 (2008).
1226 136. Wildenberg, G. A. & Murray, A. W. Evolving a 24-hr oscillator in budding yeast. *eLife* **3**,
1227 e04875 (2014).
1228 137. Dahmann, C., Diffley, J. F. X. & Nasmyth, K. A. S-phase-promoting cyclin-dependent kinases
1229 prevent re-replication by inhibiting the transition of replication origins to a pre-replicative
1230 state. *Current Biology* **5**, 1257–1269 (1995).
1231 138. Nguyen, V. Q., Co, C. & Li, J. J. Cyclin-dependent kinases prevent DNA re-replication
1232 through multiple mechanisms. *Nature* **411**, 1068–1073 (2001).
1233 139. Jacobson, M. D., Gray, S., Yuste-Rojas, M. & Cross, F. R. Testing cyclin specificity in the exit
1234 from mitosis. *Mol Cell Biol* **20**, 4483–4493 (2000).
1235 140. Kozholianko, G. SOLAR CULT OF ANCIENT UKRAINIANS. *nz* **139**, 57–64 (2018).
1236 141. Dietler, N. *et al.* A convolutional neural network segments yeast microscopy images with
1237 high accuracy. *Nat Commun* **11**, 5723 (2020).
1238 142. Jang, J. & Woolley, G. A. Directed evolution approaches for optogenetic tool development.
1239 *Biochemical Society Transactions* **49**, 2737–2748 (2021).
1240 143. Nash, A. I. *et al.* Structural basis of photosensitivity in a bacterial light-oxygen-
1241 voltage/helix-turn-helix (LOV-HTH) DNA-binding protein. *Proc. Natl. Acad. Sci. U.S.A.* **108**,
1242 9449–9454 (2011).
1243 144. Zoltowski, B. D., Motta-Mena, L. B. & Gardner, K. H. Blue light-induced dimerization of a
1244 bacterial LOV–HTH DNA-binding protein. *Biochemistry* **52**, 6653–6661 (2013).

1245 145. Glantz, S. T. *et al.* Functional and topological diversity of LOV domain photoreceptors. *Proc.*
1246 *Natl. Acad. Sci. U.S.A.* **113**, (2016).
1247 146. Swartz, T. E. *et al.* The Photocycle of a Flavin-binding Domain of the Blue Light
1248 Photoreceptor Phototropin. *Journal of Biological Chemistry* **276**, 36493–36500 (2001).
1249 147. Yee, E. F. *et al.* Signal transduction in light–oxygen–voltage receptors lacking the adduct-
1250 forming cysteine residue. *Nat Commun* **6**, 10079 (2015).
1251 148. Cui, Z., Hirata, D., Tsuchiya, E., Osada, H. & Miyakawa, T. The Multidrug Resistance-
1252 associated Protein (MRP) Subfamily (Yrs1/Yor1) of Is Important for the Tolerance to a Broad
1253 Range of Organic Anions. *Journal of Biological Chemistry* **271**, 14712–14716 (1996).
1254 149. Szczypka, M. S., Wemmie, J. A., Moye-Rowley, W. S. & Thiele, D. J. A yeast metal resistance
1255 protein similar to human cystic fibrosis transmembrane conductance regulator (CFTR) and
1256 multidrug resistance-associated protein. *Journal of Biological Chemistry* **269**, 22853–22857
1257 (1994).
1258 150. Allard, C. A. H., Decker, F., Weiner, O. D., Toettcher, J. E. & Graziano, B. R. A size-invariant
1259 bud-duration timer enables robustness in yeast cell size control. *PLoS ONE* **13**, e0209301
1260 (2018).
1261 151. Zhou, X., Vink, M., Klaver, B., Berkhout, B. & Das, A. T. Optimization of the Tet-On system
1262 for regulated gene expression through viral evolution. *Gene Ther* **13**, 1382–1390 (2006).
1263 152. Makanae, K., Kintaka, R., Makino, T., Kitano, H. & Moriya, H. Identification of dosage-
1264 sensitive genes in *Saccharomyces cerevisiae* using the genetic tug-of-war method. *Genome*
1265 *Res.* **23**, 300–311 (2013).
1266 153. Robinson, D., Place, M., Hose, J., Jochem, A. & Gasch, A. P. Natural variation in the
1267 consequences of gene overexpression and its implications for evolutionary trajectories. *eLife*
1268 **10**, e70564 (2021).

1269 154. Cravens, A., Jamil, O. K., Kong, D., Sockolosky, J. T. & Smolke, C. D. Polymerase-guided base
1270 editing enables in vivo mutagenesis and rapid protein engineering. *Nat Commun* **12**, 1579
1271 (2021).
1272 155. Skrekas, C., Limeta, A., Siewers, V. & David, F. Targeted *In Vivo* Mutagenesis in Yeast Using
1273 CRISPR/Cas9 and Hyperactive Cytidine and Adenine Deaminases. *ACS Synth. Biol.* **12**, 2278–
1274 2289 (2023).
1275 156. Yu, H. *et al.* Conserved Sequence Preferences Contribute to Substrate Recognition by the
1276 Proteasome. *Journal of Biological Chemistry* **291**, 14526–14539 (2016).
1277 157. Sari, F., Braus, G. H. & Irniger, S. A Process Independent of the Anaphase-promoting
1278 Complex Contributes to Instability of the Yeast S Phase Cyclin Clb5. *Journal of Biological*
1279 *Chemistry* **282**, 26614–26622 (2007).
1280 158. Wäsch, R. & Cross, F. R. APC-dependent proteolysis of the mitotic cyclin Clb2 is essential for
1281 mitotic exit. *Nature* **418**, 556–562 (2002).
1282 159. Fields, S. & Song, O. A novel genetic system to detect protein–protein interactions. *Nature*
1283 **340**, 245–246 (1989).
1284 160. Hu, J. H. *et al.* Evolved Cas9 variants with broad PAM compatibility and high DNA
1285 specificity. *Nature* **556**, 57–63 (2018).
1286 161. Miller, S. M. *et al.* Continuous evolution of SpCas9 variants compatible with non-G PAMs.
1287 *Nat Biotechnol* **38**, 471–481 (2020).
1288 162. Di Roberto, R. B., Chang, B. & Peisajovich, S. G. The directed evolution of ligand specificity
1289 in a GPCR and the unequal contributions of efficacy and affinity. *Sci Rep* **7**, 16012 (2017).
1290 163. Scott, B. M. *et al.* Coupling of Human Rhodopsin to a Yeast Signaling Pathway Enables
1291 Characterization of Mutations Associated with Retinal Disease. *Genetics* **211**, 597–615 (2019).
1292 164. Ladds, G., Goddard, A. & Davey, J. Functional analysis of heterologous GPCR signalling
1293 pathways in yeast. *Trends in Biotechnology* **23**, 367–373 (2005).

1294 165. Alberstein, R. G., Guo, A. B. & Kortemme, T. Design principles of protein switches. *Current*
1295 *Opinion in Structural Biology* **72**, 71–78 (2022).
1296 166. Pillai, A. *et al. De Novo Design of Allosterically Switchable Protein Assemblies*.
1297 http://biorxiv.org/lookup/doi/10.1101/2023.11.01.565167 (2023)
1298 doi:10.1101/2023.11.01.565167.
1299 167. Glasgow, A. A. *et al.* Computational design of a modular protein sense-response system.
1300 *Science* **366**, 1024–1028 (2019).
1301 168. Kretschmer, S., Perry, N., Zhang, Y. & Kortemme, T. Multi-input Drug-Controlled Switches
1302 of Mammalian Gene Expression Based on Engineered Nuclear Hormone Receptors. *ACS Synth.*
1303 *Biol.* **12**, 1924–1934 (2023).
1304 169. Jefferson, R. E. *et al.* Computational design of dynamic receptor—peptide signaling
1305 complexes applied to chemotaxis. *Nat Commun* **14**, 2875 (2023).
1306 170. Ouyang, X., Ren, H. & Huang, X. Optogenetic tools controlled by ultraviolet-B light.
1307 *aBIOTECH* **2**, 170–175 (2021).
1308 171. Rizzini, L. *et al.* Perception of UV-B by the *Arabidopsis* UVR8 Protein. *Science* **332**, 103–106
1309 (2011).
1310 172. Jang, J. *et al.* Engineering of bidirectional, cyanobacteriochrome-based light-inducible
1311 dimers (BICYCL)s. *Nat Methods* **20**, 432–441 (2023).
1312 173. Kaberniuk, A. A., Baloban, M., Monakhov, M. V., Shcherbakova, D. M. & Verkhusha, V. V.
1313 Single-component near-infrared optogenetic systems for gene transcription regulation. *Nat*
1314 *Commun* **12**, 3859 (2021).
1315 174. Bugaj, L. J. & Lim, W. A. High-throughput multicolor optogenetics in microwell plates. *Nat*
1316 *Protoc* **14**, 2205–2228 (2019).

1317 175. Meier, S. S. M., Multamäki, E., Ranzani, A. T., Takala, H. & Möglich, A. Multimodal Control
1318 of Bacterial Gene Expression by Red and Blue Light. in *Synthetic Biology* (ed. Braman, J. C.) vol.
1319 2760 463–477 (Springer US, New York, NY, 2024).
1320 176. Kolar, K., Knobloch, C., Stork, H., Žnidarič, M. & Weber, W. OptoBase: A Web Platform for
1321 Molecular Optogenetics. *ACS Synth. Biol.* **7**, 1825–1828 (2018).
1322 177. Ng, A. H. *et al.* Modular and tunable biological feedback control using a de novo protein
1323 switch. *Nature* **572**, 265–269 (2019).
1324 178. Langan, R. A. *et al.* De novo design of bioactive protein switches. *Nature* **572**, 205–210
1325 (2019).
1326 179. Shui, S., Scheller, L. & Correia, B. E. *Rationally Designed Protein Bandpass Filters for*
1327 *Controlling Cellular Signaling with Chemical Inputs*.
1328 http://biorxiv.org/lookup/doi/10.1101/2023.02.10.528077 (2023)
1329 doi:10.1101/2023.02.10.528077.
1330 180. Synthetic complete (SC) medium. *Cold Spring Harb Protoc* **2016**, pdb.rec090589 (2016).
1331 181. 5-Fluoroorotic Acid (5-FOA) Plates. *Cold Spring Harb Protoc* **2016**, pdb.rec086637 (2016).
1332 182. Gietz, R. D. & Schiestl, R. H. High-efficiency yeast transformation using the LiAc/SS carrier
1333 DNA/PEG method. *Nat Protoc* **2**, 31–34 (2007).
1334 183. Sikorski, R. S. & Hieter, P. A system of shuttle vectors and yeast host strains designed for
1335 efficient manipulation of DNA in Saccharomyces cerevisiae. *Genetics* **122**, 19–27 (1989).
1336 184. Rivera-Cancel, G., Motta-Mena, L. B. & Gardner, K. H. Identification of natural and artificial
1337 DNA substrates for light-activated LOV–HTH transcription factor EL222. *Biochemistry* **51**,
1338 10024–10034 (2012).
1339 185. Quail, P. H. Phytochromes. *Current Biology* **20**, R504–R507 (2010).
1340 186. Quail, P. H. *et al.* Phytochromes: Photosensory Perception and Signal Transduction. *Science*
1341 **268**, 675–680 (1995).

1342 187. Liu, C., Fu, Y., Lin, L., Elson, E. L. & Wang, J. Understanding Cellular Noise with Optical
1343 Perturbation and Deep Learning. (2024) doi:10.48550/ARXIV.2401.12498.
1344 188. Sharrock, R. A. The phytochrome red/far-red photoreceptor superfamily. *Genome Biol* **9**,
1345 230 (2008).
1346 189. Baron, U. & Bujard, H. Tet repressor-based system for regulated gene expression in
1347 eukaryotic cells: Principles and advances. in *Methods in Enzymology* vol. 327 401–421
1348 (Elsevier, 2000).
1349 190. Epstein, C. B. & Cross, F. R. CLB5: a novel B cyclin from budding yeast with a role in S phase.
1350 *Genes Dev.* **6**, 1695–1706 (1992).
1351 191. Orlando, D. A. *et al.* Global control of cell-cycle transcription by coupled CDK and network
1352 oscillators. *Nature* **453**, 944–947 (2008).
1353 192. Yang, X., Lau, K.-Y., Sevim, V. & Tang, C. Design Principles of the Yeast G1/S Switch. *PLoS*
1354 *Biol* **11**, e1001673 (2013).
1355 193. Lengronne, A. & Schwob, E. The Yeast CDK Inhibitor Sic1 Prevents Genomic Instability by
1356 Promoting Replication Origin Licensing in Late G1. *Molecular Cell* **9**, 1067–1078 (2002).
1357 194. Zhu, Y. O., Siegal, M. L., Hall, D. W. & Petrov, D. A. Precise estimates of mutation rate and
1358 spectrum in yeast. *Proc. Natl. Acad. Sci. U.S.A.* **111**, (2014).
1359
1360

Acknowledgments

We thank Roxane Dervey for help with strain construction and media preparation; Dr. Kyle Douglass and Prof. Suliana Manley for help with the laser experiments; Prof. Peter Quail, Prof. Hana El-Samad, and Dr. Brian Graziano for providing PhyB-Pif3 strains and constructs; Prof. José L. Avalos and Dr. Evan Zhao for providing the *EL222* plasmid; Prof. Andrew Murray for providing the *pol3-L523D* strain; and Dr. Enrico Tenaglia for help with molecular cloning. We thank the mechanical and electronics workshops of the Institute of Physics in the Cubotron building at EPFL for help building the hardware for optogenetic stimulation. We acknowledge support for VG, ML, and SJR provided by SNSF grants CRSK-3_190526 and 310030_204938 awarded to SJR.

Author contributions

VG and SJR designed the experiments and analyzed the data. VG constructed the strains used for evolution. VG performed the directed evolution experiments. VG and ML characterized the evolved variants by fluorescence microscopy. VG and SJR wrote the manuscript. SJR supervised the work and acquired funding.

Competing interests

VG and SJR have filed a provisional patent application for the method reported in this manuscript through EPFL.

1379 # Supplementary Material

1380 ## Supplementary Note 1: List of previous multiple-goal continuous
1381 directed evolution campaigns

Publication	Molecular target	Details	Host	Ref.
Continuous directed evolution of DNA-binding proteins to improve TALEN specificity Hubbard et al., 2015	TALENs	Based on the PACE platform[14] Positive selection: DNA binding domain of TALENs coupled to phage propagation by way of bacterial RNA polymerase Negative selection: Promiscuous phage activity coupled to pIII-neg that inhibits phage propagation	*E. coli*	19
Evolution of a split RNA polymerase as a versatile biosensor platform Pu et al., 2017	T7 RNAP	Based on the PACE platform[14] Positive selection: Desired interaction between the halves of RNAP linked to phage propagation Negative selection: Interaction with alternative domains counterselected by linking promiscuous activity to dominant negative pIII-neg	*E. coli*	20
Contingency and chance erase necessity in the experimental evolution of ancestral proteins Xie et al., 2021	BCL-2 coregulators	Based on the PACE platform[14] Positive selection: The interaction of interest drives the expression of pIII necessary for phage propagation Negative selection: Unwanted interaction is counterselected by linking its activity to dominant negative pIII-neg	*E. coli*	21
Directed Evolution and Substrate Specificity Profile of Homing Endonuclease I-SceI Doyon et al., 2006	I-SceI	Positive selection: Endonuclease activity of I-SceI rescues the host cell by digesting a plasmid with a toxic gene (*ccdB*) Negative selection: Promiscuous substrate recognition suppressed using an antibiotic-resistance plasmid that must not be cut by I-SceI	*E. coli*	22
Engineered CRISPR-Cas9 nucleases with altered PAM specificities Kleinstiver et al., 2015	Cas9	Positive selection: Survival requires Cas9-mediated cleavage of a plasmid harboring a toxic gene Negative selection: Unwanted recognition of PAM sequences is suppressed using an antibiotic resistance plasmid whose cleavage by Cas9 leads to cell death	*E. coli*	23
Directed evolution of CRISPR-Cas9 to increase its specificity Lee et al., 2018	Cas9	Positive selection: Survival requires Cas9-mediated cleavage of a plasmid harboring a toxic gene Negative selection: Off-target cleavage is suppressed by introducing potential recognition sequences into *E. coli* genome that if cut lead to cell death	*E. coli*	24
A bacterial dual positive and negative selection system for dCas9 activity	Cas9	Positive selection: dCas9- and LacI-mediated derepression of antibiotic resistance genes Negative selection: dCas9-mediated repression of essential genes	*E. coli*	25

Spisak et al., 2022				
Engineered dual selection for directed evolution of SpCas9 PAM specificity Goldberg et al., 2021	Cas9	Positive selection: dCas9-mediated expression of *HIS3* auxotrophic gene, essential in media without histidine Negative selection: off-target binding leads to repression of *HIS3*	*E. coli*	[26]
A highly specific SpCas9 variant is identified by in vivo screening in yeast Casini et al., 2018	Cas9	Positive selection: On-target cleavage leads to reconstitution of functional auxotrophic marker *TRP1* Negative selection: Off-target cleavage leads to reconstitution of *ADE2*, which causes color change of yeast colony	Budding yeast	[27]

Supplementary Note 2: List of previous selection/counterselection directed evolution campaigns

Publication	Molecular target	Selection mechanism	Organism	Timing of selection cycles	Mutagenesis	Selection environ-ment	Ref.
Robust and flexible platform for directed evolution of yeast genetic switches Tominaga et al., 2021	Tet-ON system and biosensors for DAPG and Camphor	Positive selection: *BLE* expression (Zeocin resistance) Negative selection: hsvTK activity in the presence of specific substrates leads to toxic products	Budding yeast	24 h of negative selection followed by 24 h induction and final positive selection for 24 h	Error-prone PCR	Liquid	[38]
Ribozyme-Based Aminoglycoside Switches of Gene Expression Engineered by Genetic Selection in *S. cerevisiae* Klauser et al., 2015	RNA switches	Positive selection: *HIS3* auxotrophic marker expression Negative selection: *URA3* expression in medium with 5-fluoroorotic acid (5-FOA)	Budding yeast	Not specified	Randomized library	Solid	[39]
Engineering prokaryotic transcriptional activators as metabolite biosensors in yeast Skjoedt et al., 2016	Transcriptional biosensor based on LTTR family of proteins	FACS (Fluorescence activated cell sorting)-based screening	Budding yeast	Cells grown for 24 h without inducer were subjected to negative selection followed by a 24 h induction and positive selection	Error-prone PCR	Liquid	[40]
Evolution-guided engineering of small-molecule biosensors Snoek et al., 2020	Transcriptional sensors for *cis,cis*-muconic acid	FACS-based screening	Budding yeast	Single round of FACS-selection for desired phenotype with cells grown under inducing or non-inducing conditions for 22 h	Error-prone PCR	Liquid	[41]

Photo-sensitive degron variants for tuning protein stability by light Usherenko et al., 2014	Photosensitive degron	Manual screen for different fluorescence in darkness/light	Budding yeast	Replicas of colonies screened under inducing and non-inducing conditions separately after 24 h of growth	Error-prone PCR	Solid	[42]
A Yeast System for Discovering Optogenetic Inhibitors of Eukaryotic Translation Initiation Lu et al., 2019	Optogenetic inhibitors of translation	Positive selection based on translation inhibition	Budding yeast	Replicas of colonies screened under inducing and non-inducing conditions separately after 2 days of growth	Error-prone PCR	Solid	[43]
A light- and calcium-gated transcription factor for imaging and manipulating activated neurons Wang et al., 2017	Light- and calcium-gated transcription factor	FACS-based screen	Budding yeast	Six rounds of alternating positive and negative selection with 2-3 days of growth between each round	Error-prone PCR	Liquid	[44]
Yeast Two-Hybrid Screening of Photoswitchable Protein–Protein Interaction Libraries Woloschuk et al., 2020	Proteins that interact with photoswitcha-ble proteins	Positive selection based on yeast-two-hybrid driven expression of *HIS3* auxotrophic marker	Budding yeast	Positive selection for 72 h after the transformation followed by separate screens of replicas under inducing and non-inducing conditions grown for 48 h	Site-directed mutagenesis	Solid	[45]
Optimized second-generation CRY2-CIB dimerizers and photoactivatable Cre recombinase Taslimi et al., 2016	CRY2	Dual selection based on yeast-two-hybrid driven expression of *URA3* gene on -uracil (positive) or +5-FOA plates (negative)	Budding yeast	For identifying light-sensitized variants, cells were subjected to low light on -uracil plates and then replica-plated in darkness onto 5-FOA plates. For identifying low-leakiness variants, cells were subjected to selection under low light on 5-FOA plates and then replica-plated onto -uracil plates under a high-light regime. Timing not fully specified.	Error-prone PCR	Solid	[46]
Creating Red Light-Switchable Protein Dimerization Systems as Genetically Encoded Actuators with High Specificity Huang et al., 2020	Binders of bacterial phytochrome	The library enriched by phage display was further screened in budding yeast using the yeast two-hybrid method	Budding yeast	Growth of budding yeast under positive selection conditions for 4-5 days followed by separate screening of replica colonies under inducing and non-inducing conditions for 24 h to exclude constitutively active mutants	Randomized library	Solid	[47]
Engineering an	LOV domains	Positive selection:	Phage	Four rounds of the	Rationally	*Ex vivo*	[48]

improved light-induced dimer (iLID) for controlling the localization and activity of signaling proteins Guntas et al., 2015		binding under light Negative selection: elution in darkness	display	following steps: 1 h light induction, selection, 10 min in darkness, and counter-selection	designed library		
Discovering Selective Binders for Photoswitchable Proteins Using Phage Display Reis et al., 2018	Binders of PYP and LOV2	Selection for binding of either darkness- or light-adapted form of the protein, with washouts designed to reduce constitutive binding	Phage display *E. coli* (used for protein expres-sion)	Three rounds of selection and counterselection with 1 h exposure to light or 1 h in darkness for proteins to adopt their light- or dark-states, respectively.	Site-directed mutagenesis	*Ex vivo*	[49]
LOVTRAP: an optogenetic system for photoinduced protein dissociation Wang et al., 2016	LOV domains	mRNA display (Selection for binding in darkness with washouts designed to reduce constitutive binding)	*E. coli* (used for protein expressio n)	12 rounds of selection. Timing not specified.	Randomized library	*Ex vivo*	[50]
Fluorescence Imaging-Based High-Throughput Screening of Fast- and Slow-Cycling LOV Proteins Kawano et al., 2013	LOV domains	Manual screen of mutant colonies	*E. coli*	Transient induction followed by timelapse imaging of bacterial colonies for three hours	Site-directed mutageneis	Solid	[51]
Directed evolution of a genetic circuit Yokobayashi et al., 2002	Logic gate based on constitutive bacterial regulators	Manual screen of colonies	*E. coli*	Not specified	Error-prone PCR	Solid	[52]
Evolving Orthogonal Suppressor tRNAs To Incorporate Modified Amino Acids Maranhao and Ellington, 2017	tRNA	Positive selection: compartmentalized partnered replication (CPR) Negative selection: incorporation of toxic *p*-Cl-phenylalanine (p-Cl-Phe)	*E. coli*	Three rounds of CPR, each including 3 h of growth, then 4 h of incubation with p-Cl-Phe for negative selection, followed by a final round of CPR	Randomized library	Liquid	[53]
Enhancing the performance of Magnets photosensors through directed evolution Baumschlager et al., 2022	LOV domains	FACS-based selection	*E. coli*	For each selection step, cells were grown in inducing or non-inducing conditions for 4 h. Three rounds of selection in total: two positive with one negative in-between	Error-prone PCR	Liquid	[54]
Escherichia coli "Marionette" strains with 12 highly optimized small-molecule sensors Meyer et al., 2019	12 prokaryotic chemically-responsive biosensors	Positive selection: expression of DNA Polymerase for compartmentalized partnered replication Negative selection:	*E. coli*	Alternating negative selection for 12-16 h, followed by positive selection for 4 h, with 4-23 total rounds of selection	Randomized library of biosensors with intermittent library shuffling	Liquid	[55]

		incorporation of lethal *p*-Cl-phenylalanine (p-Cl-Phe)					
A nucleoside kinase as a dual selector for genetic switches and circuits Tashiro et al., 2011	Logic gate protein circuits	Positive and negative selection based on activity of *hsvTK* gene	*E. coli*	12-15 h of positive selection followed by 12 h of negative selection	N/A	Liquid and solid	[56]
Engineering an allosteric transcription factor to respond to new ligands Taylor et al., 2016	LacI	Positive selection: FACS of fluorescently labeled cells Negative selection: Expression of the toxin importer *tolC* gene	*E. coli*	Overnight negative selection followed by a FACS-based positive selection	Rationally designed mutation library combined with error-prone PCR	Liquid	[57]
AraC Regulatory Protein Mutants with Altered Effector Specificity Tang et al., 2008	AraC	FACS-based selection	*E. coli*	Positive selection after overnight induction followed by negative selection (no timing specified for negative selection)	Error-prone PCR	Liquid	[58]
Directed evolution of AraC for improved compatibility of arabinose- and lactose-inducible promoters Lee et al., 2007	AraC	FACS-based positive selection	*E. coli*	Only positive selection with FACS after 6 h of induction	Error-prone PCR	Liquid	[59]
Directed Evolution of the Quorum-Sensing Regulator EsaR for Increased Signal Sensitivity Shong et al., 2013	EsaR	Semi-automated screen using pin replicator and luminescence measurements	*E. coli*	24 h of incubation under non-inducing conditions, then negative selection, followed by overnight incubation under inducing conditions and positive selection for 24 h	Error-prone PCR	Solid	[60]
Dual selection of a genetic switch by a single selection marker Nomura and Yokobayashi, 2007	*lac* promoter	Proof of principle that a single selection marker (*tetA*) can be used for both positive and negative selection. *tetA* is essential for tetracycline resistance but renders cells more sensitive to $NiCl_2$	*E. coli*	20-24 h in $NiCl_2$, followed by a 1.5 h incubation period and 17-24 h of selection by tetracycline	N/A	Solid	[61]
An efficient platform for genetic selection and screening of gene switches in *Escherichia coli* Muranaka et al., 2009	Thiamine riboswitches	Positive and negative selection based on *tetA* expression	*E. coli*	8 h of induction, then 24 h of positive selection, followed by washout, 8 h of growth under non-inducing conditions and 24 h of negative selection	Randomized library	Liquid	[62]
Engineering Complex	Theophylline	Positive and negative	*E. coli*	Two cycles of	Rationally	Solid	[63]

Riboswitch Regulation by Dual Genetic Selection Sharma et al., 2008	and Thiamine riboswitches	selection based on *tetA* expression		selection for each of the input combinations. Each selection step lasted 24 h	constructed library		
Engineering of temperature- and light-switchable Cas9 variants Ritches et al., 2013	dCas9	FACS-based selection	*E. coli*	Positive selection followed by negative selection with induction time dependent on the temperature (4-19 h)	Rationally designed library	Liquid	[64]
Rapid and Liquid-Based Selection of Genetic Switches Using Nucleoside Kinase Fused with Aminoglycoside Phosphotransferase Tominaga et al., 2015	Lux promoter variants	Positive selection based on two different antibiotic resistance genes Negative selection based on *hsvTK* gene	*E. coli*	Negative selection overnight followed by a washout and 4-6 h of positive selection in the presence of the inducer	Site-directed mutagenesis	Liquid	[65]
Rapid Diversification of BetI-Based Transcriptional Switches for the Control of Biosynthetic Pathways and Genetic Circuits Saeki et al., 2016	Choline-inducible transcription factor BetI	Positive selection based on two different antibiotic resistance genes Negative selection based on *hsvTK* gene	*E. coli*	1 h of incubation, then 3 h of negative selection followed by 1 h of incubation and 3 h of positive selection. Depending on the desired outcome, the inducer was added during the incubation time, either before positive or negative selection	Error-prone PCR	Liquid	[66]
Evolutionary Design of Choline-Inducible and -Repressible T7-Based Induction Systems Ike et al., 2015	Choline-inducible transcription factor BetI	Screen for and against fluorescence under inducing and non-inducing conditions	*E. coli*	Selection of colonies that fluoresce under inducible conditions followed by a screen of liquid culture replicates separately under inducing and non-inducing conditions to exclude constitutive variants. Each incubation step was performed overnight.	Error-prone PCR	Solid	[67]
Directed evolution of protein switches and their application to the creation of ligand-binding proteins Guntas et al., 2005	Beta-lactamase	Selection of cells that survive under maltose and beta-lactamase antibiotic targets	*E. coli*	Cells selected for survival on plates containing maltose and ampicillin were further screened for maltose-dependence. Timing not specified.	Random domain insertion and random circular permutation	Solid	[68]
Directed evolution of the autoinducer selectivity of *Vibrio fischeri* LuxR Tashiro et al., 2016	LuxR	Dual selection based on the *hsvTK* gene	*E. coli*	2 h of negative selection, followed by a washout, induction of 6 h and positive selection of 20 h	Site-directed mutagenesis	Liquid	[69]

Directed evolution of a synthetic phylogeny of programmable Trp repressors Ellefson et al., 2018	TrpR	Dual selection based on compartmentalized partnered replication	*E. coli*	Variants obtained from the first CPR round of positive selection were cloned into another plasmid that allowed negative CPR selection. Before each CPR, cells were grown for 1 h, followed by 4 h of growth in inducing conditions	Randomized library	Liquid	[70]
Engineered systems of inducible anti-repressors for the next generation of biological programming Groseclose et al., 2020	Several classes of antirepressors	FACS-based selection	*E. coli*	Positive selection followed by negative selection. Timing not specified.	Error-prone PCR	Liquid	[36]

Supplementary Note 3: El222 optogenetic system

El222 is a transcription factor from marine bacterium *Erythrobacter litoralis*.[144] El222 has been adapted for use in eukaryotes by way of a tandem fusion of the prokaryotic El222 transcription factor, a nuclear localization signal, and the VP16 transcriptional activation domain. In darkness, the interaction of the helix-turn-helix (HTH) DNA binding domain with DNA is sterically hindered by the light-sensing LOV-domain[143]. Upon blue light illumination, a covalent bond is formed between the Cys-75 residue and the flavin chromophore[146]. (All references to mutant residue numbers in El222 are given with respect to bacterial El222 to match the numbering used in previous work[88,143,144].) This leads to a conformational change, which dislocates the Jα helix of the LOV domain. Subsequently, the protein forms a homodimer and binds to the DNA substrate using its exposed HTH domain. In the absence of blue light, the protein reverts to its ground state. For brevity, we refer to the promoter consisting of 5 El222 binding sites[184] upstream of a minimal eukaryotic promoter as *LIP*.

1400 # Supplementary Note 4: PhyB-Pif3 optogenetic system

1401 Phytochromes are photosensors in plants, bacteria, and fungi[185]. Phytochrome B and its
1402 interaction partner Pif3 are used by plants to adapt gene expression to environmental light
1403 conditions[186].

1404 The light-inducible PhyB-Pif3 interaction has been extensively used in organisms other than
1405 plants[106–109]. By fusing one protein to PhyB and another to Pif3, one can induce protein-protein
1406 interactions in a temporarily and spatially precise manner, for example, in order to sequester
1407 proteins to specific cellular compartments[107]. In the yeast two-hybrid version of the system, it is
1408 used for light-inducible transcriptional control in budding yeast.[108, 187] Typically, PhyB and Pif3 are
1409 fused to the Gal4 DNA binding domain and the Gal4 transcriptional activation domain,
1410 respectively.[108] When bound to its chromophore and activated by red light (≈650 nm), PhyB binds
1411 Pif3, thereby, bringing the transcriptional activation and DNA binding domains close together,
1412 which leads to the expression of the *GAL* family of genes. In the presence of far-red light (≈ 740
1413 nm) or prolonged darkness, PhyB changes conformation again and dissociates from Pif3.

1414 The photoreceptive core of the PhyB protein contains a linear tetrapyrrole chromophore.[188] In
1415 plants, this chromophore is phytochromobilin. However, phytochromobilin is not produced in
1416 many model organisms. Thus, to use PhyB-Pif3, one adds phycocyanobilin (PCB), which is a
1417 precursor of phytochromobilin in plants and a chromophore in algal phytochromes, to the
1418 incubation medium prior to optogenetic experiments. It has been shown that bacterial and fungal
1419 phytochromes can carry biliverdin, another tetrapyrrole molecule, as a chromophore.[188]

1420

1421 # Supplementary Note 5: Tetracycline-regulated gene expression
1422 systems

1423 Tetracycline-responsive systems, originally identified in bacteria as part of a feedback loop that
1424 mediates resistance to the antibiotic tetracycline, are widely used for controlling transcription. The
1425 system is made up of the tTA regulator, which binds the *tetO* DNA sequence. In its original form,
1426 tTA is part of the Tet-Off system that is inhibited by tetracycline or the closely related molecule
1427 doxycycline[189]. Mutations that reverse tTA activity with respect to the inducer have been used to
1428 construct rtTA.[115] To function as a transcriptional activator in eukaryotes, rtTA is typically fused to
1429 the VP16 transactivation domain. To construct an inducible eukaryotic promoter, the binding sites
1430 for rtTA, *tetO*, are placed next to a minimal promoter. However, this system, called the Tet-On
1431 system, exhibits high basal activity in the absence of the inducer. To circumvent this, we fused the
1432 PEST degron to rtTA, which leads to increased degradation of rtTA.

1433

1434 # Supplementary Note 6: Summary of cell cycle biology relevant to
1435 optovolution

1436 ## Wild-type cell cycle control

1437 In this note, we briefly summarize the wild-type model of cell cycle control in budding yeast.[131] In
1438 the next section, we focus on how the cell cycle runs in the Dajbog strains.

1439 At the biochemical level, the rhythm of the cell-cycle oscillator is predominantly generated by a
1440 negative feedback loop[129]. In this loop, cyclin-dependent kinase (CDK) and the anaphase-
1441 promoting complex/cyclosome (APC/C) alternate in activity and drive cell cycle progression.

1442 In budding yeast, there is a single cyclin-dependent kinase, Cdk1 (also known as Cdc28). Processes
1443 that Cdk1 controls include the transcription of hundreds of cell cycle-periodic genes, DNA
1444 replication, spindle pole body duplication, and spindle formation. Activity and specificity of Cdk1
1445 towards different substrates is mainly regulated through its interaction with regulatory proteins
1446 called cyclins. Different cyclins generally promote distinct cell-cycle events and are expressed at
1447 different stages of the cell cycle. In *S. cerevisiae*, cyclins are commonly classified into four groups:
1448 G1, G1/S, S, and M cyclins. Each cyclin-Cdk complex promotes the activation of the next group of
1449 cyclins.

1450 The G1 cyclin Cln3 activates G1/S cyclins Cln1 and Cln2 and has a role in cell-cycle entry in
1451 response to growth. Cln1-3 are responsible for the initiation of formation of the daughter cell and
1452 expression of the 100s of genes of the Start regulon. At the onset of S phase, levels of S cyclins
1453 Clb5 and Clb6 rise. Their association with Cdk1 is primarily responsible for the initiation of DNA
1454 replication by triggering the activation of origins of replication. Approaching mitosis, the
1455 concentrations of the remaining B-type cyclins increase. In budding yeast, there are four such
1456 cyclins, Clb1, Clb2, Clb3, and Clb4. Their association with Cdk1 enables assembly of the mitotic
1457 spindle and attachment of chromosomes to the spindle.

1458 In order to enable mitotic exit and reset the state of the cell for new cell cycles, cyclins have to be
1459 inactivated. While the activity G1/S cyclins is brought down by degradation and inhibition of the
1460 transcription factor SBF, S and M phase cyclins are not degraded until anaphase. At least two
1461 different mechanisms help repress Clb cyclin activity. The first one is through the activation of
1462 APC/C by the proteins Cdc20 and Cdh1. APC/C is a ubiquitin ligase complex that marks cyclins for
1463 degradation by the proteasome. The second mechanism is through the protein Sic1, which
1464 stoichiometrically inhibits Cdk1-Clb complexes, thereby effectively reducing their activity.

1465 ## Rewired cell cycle control in the Dajbog strains

1466 Although cyclins are specialized for certain phases of the cell cycle, the functions of some cyclins
1467 overlap. For example, when overexpressed, S phase cyclin Clb5 can initiate budding in a *cln1-3Δ*

1468 block[190]. Similarly, the M-phase cyclins Clb1[191]or Clb2[127]can assume the roles of all other Clb
1469 cyclins in a *clb1-6Δ* background. Endogenous *CLB3-6* genes also suffice for cell cycle start when the
1470 Clb-cyclin inhibitor *SIC1* is deleted, rendering *cln1-3Δ sic1Δ* cells viable[133].

1471 While G1/S cyclin and S cyclin expression initiates at about the same time under the control of
1472 transcription factors Sbf and Mbf[131], respectively, S cyclins are inactive until G1/S cyclins have
1473 sufficiently degraded Sic1 and Cdh1. Thus, in wild-type cells, although *CLN2* and *CLB5* are
1474 simultaneously transcriptionally activated, there is a delay between G1/S-Cdk and S-Cdk
1475 activity[131,192]. We expect this delay to persist in Dajbog1 cells. Deleting *SIC1* in Dajbog2 cells is
1476 expected to cause an increase in chromosomal rearrangements due to premature S-Cdk activity[193]
1477 but this did not noticeably interfere with our directed evolution experiments.

1478 Clb5-Cdk1 leads to the firing of origins of replication in S phase. Overexpression of destruction box
1479 deficient Clb5db in galactose medium arrests the cell cycle by inhibiting the formation of pre-
1480 replicative origins, a process known as origin of replication relicensing[137–139]. This represents the
1481 expected mechanism for the lethality of *CLB5* overexpression in glucose medium. This observation
1482 led us to further sensitize Dajbog1 cells to continuous Clb5 activity by deleting *SIC1*, resulting in
1483 Dajbog2 strains.

1484

1485 # Supplementary Figures

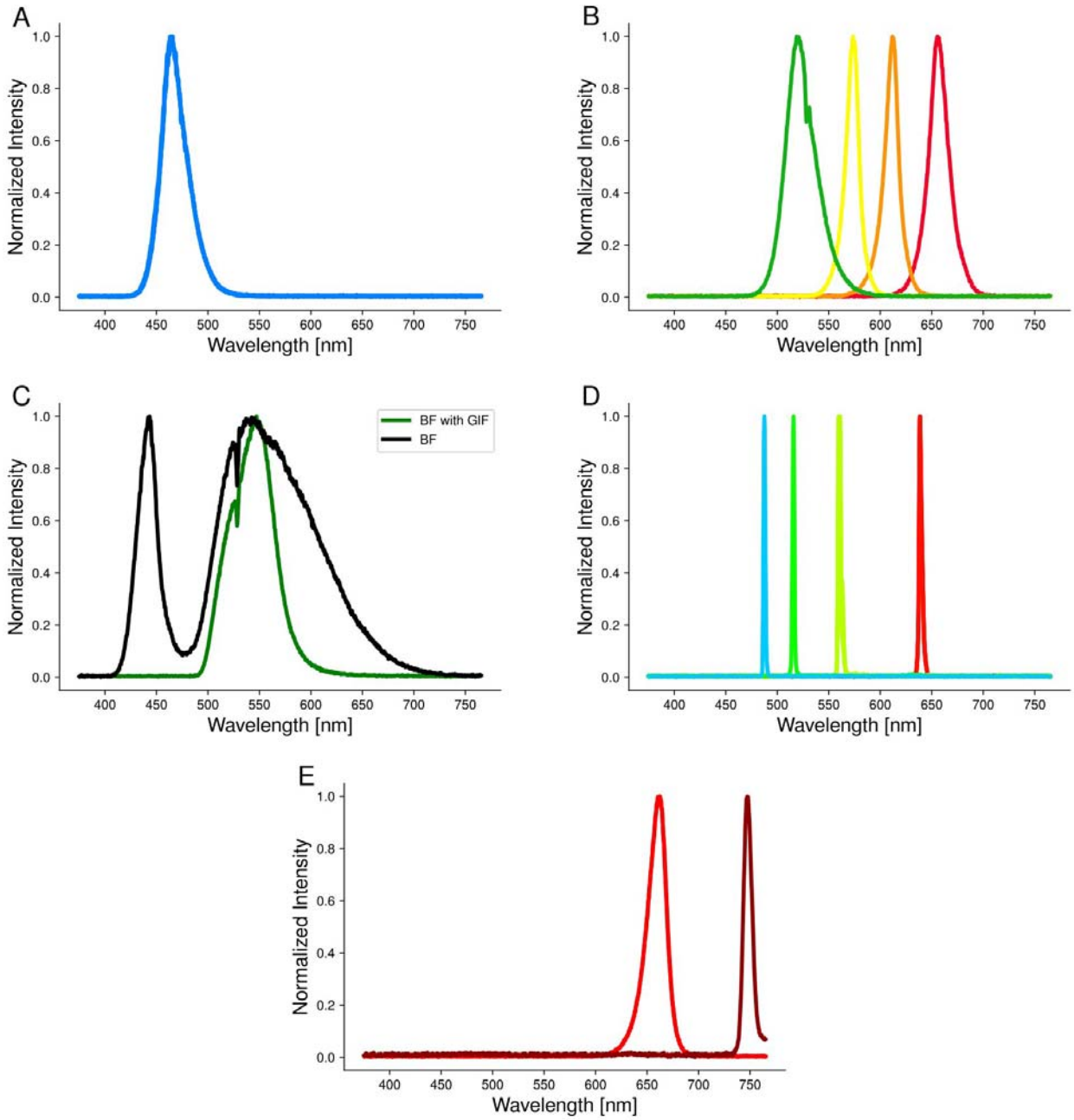

1486

1487 Supplementary Fig. 1. Emission spectra of light sources used. All reported intensities are total intensities and are for
1488 the location of the agar plates. A: Blue LED panel used for evolving and inducing El222 and its variants (light intensity
1489 8.3 mW/cm^2). B: LEDs used to evolve color-shifted El222 variants from left to right: 24 mW/cm^2, 0.12 mW/cm^2, 2.6
1490 mW/cm^2, 0.46 mW/cm^2. C: Diascopic LED light used for inducing El222 and its variants for microscopy. The black plot
1491 represents the spectrum of the brightfield (BF) light and the green plot is the spectrum of the same light filtered using
1492 a green interference filter (GIF). BF with GIF is used for inducing color-shifted mutants of El222 for timelapse
1493 microscopy. The intensities of the light are: 8.4 mW/cm^2 for BF set to 20% of the maximal power, 97 mW/cm^2 for BF
1494 set to 80% of maximal power, and 26 mW/cm^2 for BF 80% with GIF. D: Lasers used for characterizing color-shifted
1495 variants of El222. The effective light intensity of the lasers was adjusted to be the same across lasers using neutral

1496 density filters and by adjusting the duty-cycle regime of the pulsing laser light. The power intensity was 3.5 mW/cm^2
1497 for all lasers. E: Red and far-red LEDs used for switching the PhyB-Pif3 system. Light intensity of the red LEDs is 36
1498 mW/cm^2, and the light intensity of the far-red LEDs is 26 mW/cm^2.

1499

1500

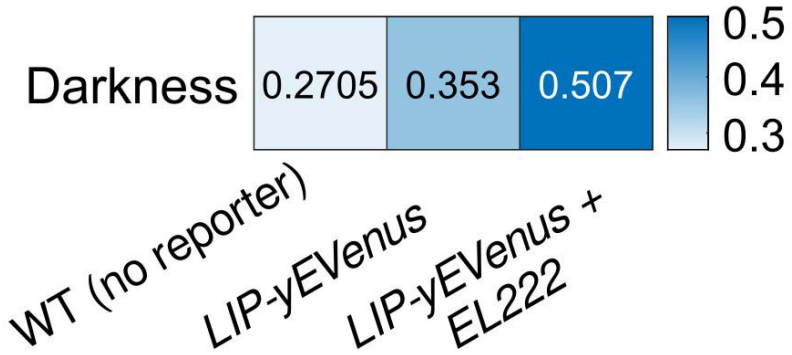

1501

1502 Supplementary Fig. 2. Baseline leakiness of the reporter sets the minimum leakiness attainable in optovolution.
1503 Comparison of fluorescence in no-reporter (WT), reporter-only (*LIP-yEVenus*), and reporter plus El222 strains (*LIP-*
1504 *yEVenus + EL222*) in darkness. Cells that contain a transcriptional reporter for El222 (*LIP-yEVenus*) but not the
1505 transcription factor (e.g., *PGK1pr-EL222*) showed elevated fluorescence compared to wild-type budding yeast cells.
1506 This suggests that other transcription factors might weakly drive the transcription from *LIP* and set the lower bound
1507 for leakiness of *LIP*. The leakiness reported for all El222 variants is the difference between the reporter-only and the
1508 reporter plus variant strains. Numbers of analyzed cells are given in the Supplementary Table 11.

1509

1510

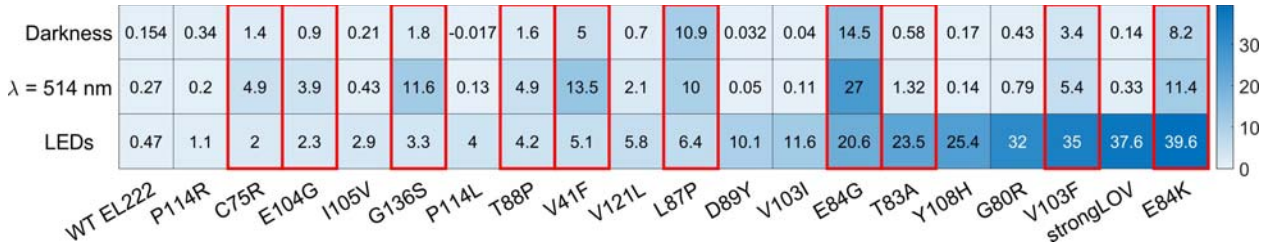

Supplementary Fig. 3. Level of activity of El222 mutants obtained in the color-shift campaign in darkness, activated by a 514 nm laser (second row), or in the presence of the green-to-red LEDs used for the campaign (third row). These measurements showed that only some of the mutants are responsive to 514 nm light. Other mutants may merely have evolved to be more sensitive to the small-wavelength tail of our green LEDs, which is why we excluded them from further analysis. We only further characterized the mutants that are substantially activated by 514 nm light. In addition, we included the L87P mutant which showed unexpected behavior by turning off in the presence of the LEDs. The values are given in percentages of 1 maxGAL1[88]. Numbers of analyzed cells are given in Supplementary Table 12.

1521 # Supplementary Tables

1522 Supplementary Table 1. Plasmids used in the study

Plasmid name	Insert	Type of plasmid	Yeast selection marker	Bacterial selection marker	Source of the plasmid
EZL105	*PGK1pr-EL222*	For integration in a single copy	*CgHIS3*	*AmpR*	Ref. [93]
pVG117	*PGK1pr-EL222 (Asp18Tyr, Val139Leu)*	For integration in a single copy	*CgHIS3*	*AmpR*	This study
pVG118	*PGK1pr-EL222 (Asp18Tyr)*	For integration in a single copy	*CgHIS3*	*AmpR*	This study
pVG119	*PGK1pr-EL222 (Val139Leu)*	For integration in a single copy	*CgHIS3*	*AmpR*	This study
pVG135	*PGK1pr-EL222 (Lys99Glu)*	For integration in a single copy	*CgHIS3*	*AmpR*	This study
pVG136	*PGK1pr-EL222 (Pro165Ser)*	For integration in a single copy	*CgHIS3*	*AmpR*	This study
pVG137	*PGK1pr-EL222 (Val201Leu)*	For integration in a single copy	*CgHIS3*	*AmpR*	This study
pVG120	*PGK1pr-EL222 (Asp89Tyr)*	For integration in a single copy	*CgHIS3*	*AmpR*	This study
pVG147	*PGK1pr-EL222 (Gly94Cys)*	For integration in a single copy	*CgHIS3*	*AmpR*	This study
pVG122	*PGK1pr-strongLOV*	For integration in a single copy	*CgHIS3*	*AmpR*	Ref. [88]
pVG143	*PGK1pr-EL222 (Leu87Ile)*	For integration in a single copy	*CgHIS3*	*AmpR*	This study
pVG123	*PGK1pr-EL222 (Ala157Val)*	For integration in a single copy	*CgHIS3*	*AmpR*	This study
pVG286	*PGK1pr-EL222 (Gly80Glu)*	For integration in a single copy	*CgHIS3*	*AmpR*	This study
pVG121	*PGK1pr-EL222 (Gly82Val)*	For integration in a single copy	*CgHIS3*	*AmpR*	This study
pVG124	*PGK1pr-EL222 (Thr83Ser)*	For integration in a single copy	*CgHIS3*	*AmpR*	This study
pVG310	*PGK1pr-AQTrip* (yeast codon-optimized)	For integration in a single copy	*CgHIS3*	*AmpR*	This study
pVG150	*PGK1pr-EL222*	For integration in a	*CgHIS3*	*AmpR*	This study

	(Ser137Asn)	single copy			
pVG144	*PGK1pr-EL222 (Val121Met)*	For integration in a single copy	*CgHIS3*	*AmpR*	This study
pVG178	*PGK1pr-EL222 (Glu84Lys)*	For integration in a single copy	*CgHIS3*	*AmpR*	This study
pVG298	*PGK1pr-EL222 (Thr83Ala)*	For integration in a single copy	*CgHIS3*	*AmpR*	This study
pVG131	*PGK1pr-EL222 (Glu104Gly)*	For integration in a single copy	*CgHIS3*	*AmpR*	This study
pVG142	*PGK1pr-EL222 (Cys75Arg)*	For integration in a single copy	*CgHIS3*	*AmpR*	This study
pVG132	*PGK1pr-EL222 (Thr88Pro)*	For integration in a single copy	*CgHIS3*	*AmpR*	This study
pVG138	*PGK1pr-EL222 (Gly136Ser)*	For integration in a single copy	*CgHIS3*	*AmpR*	This study
pVG126	*PGK1pr-EL222 (Val103Phe)*	For integration in a single copy	*CgHIS3*	*AmpR*	This study
pVG139	*PGK1pr-EL222 (Val41Phe)*	For integration in a single copy	*CgHIS3*	*AmpR*	This study
pVG252	*PGK1pr-EL222 (Leu87Pro)*	For integration in a single copy	*CgHIS3*	*AmpR*	This study
pVG134	*PGK1pr-EL222 (Glu84Gly)*	For integration in a single copy	*CgHIS3*	*AmpR*	This study
pVG101	*PGK1pr-EL222, LIP-CLN2, LIP-CLB5*	For integration	*NatMX*	*AmpR*	This study
pVG104	*ADH1pr-PHYB, ADH1pr-PIF3, GAL1-CLB5*	For integration	*NatMX*	*AmpR*	This study
pVG329	*YOR1 3'UTR and YOR1 5'UTR*	For ORF replacement	*HphMX*	*AmpR*	This study
pVG84	*GAL1pr-CLN2*	For integration	*PatMX*	*AmpR*	This study
pVG48	*GAL1pr-yEVenus-PEST*	For integration in a single copy	*URA3*	*AmpR*	Ref. [88]
pVG9	*LIP-yEVenus-PEST*	For integration in a single copy	*URA3*	*AmpR*	Ref. [88]
pVG175	*LIP-ymScarletI*	For integration in a single copy	*URA3*	*AmpR*	This study
pVG176	*LIP-ymScarletI-PEST*	For integration in a single copy	*URA3*	*AmpR*	This study
pVG295	*PGK1pr-EL222, LIP-PEST-rtTA, tetOpr-CLN2*	For integration	*NatMX*	*AmpR*	This study

pRD-TW1 (pRD13)	*MET3pr-CLN2, CLB5pr-CLB5*	*CEN/ARS*	*URA3*	*AmpR*	This study
pRD70	*tetOpr-CLB5*	For integration	*PatMX*	*AmpR*	This study
pVG336	*PGK1pr-PEST-rtTA*	For integration in a single copy	*HIS3*	*AmpR*	This study
pVG337	*PGK1pr-PEST-rtTA (Phe67Cys)*	For integration in a single copy	*HIS3*	*AmpR*	This study
pVG338	*PGK1pr-PEST-rtTA (Arg253His)*	For integration in a single copy	*HIS3*	*AmpR*	This study
pVG188	*PGK1pr-EL222, LIP-CLN2*	For integration in a single copy	*NatMX*	*AmpR*	This study
pVG189	*PGK1pr-EL222, LIP-CLB5*	For integration in a single copy	*NatMX*	*AmpR*	This study
pVG70	*PGK1pr-EL222, LIP-CDC20*	For integration	*NatMX*	*AmpR*	This study
pVG15k	*PGK1pr-EL222, LIP-CLB2kd*	For integration	*NatMX*	*AmpR*	This study
pVG47	*tetOpr-yEVenus-PEST*	For integration in a single copy	*URA3*	*AmpR*	Ref. [88]

1525 Supplementary Table 2. Strains used in the study

Strain name	Genotype	Source
yVG602	*cln1,3Δ cln2Δ::MET3pr-CLN2 clb1Δ clb2Δ::GALL-CLB2::URA3 HTB2::HTB2-mCherry::HIS3 PGK1pr::PGK1pr-EL222, LIP-CLB2::NatMX*	This study
yVG173	*clb1Δ clb2Δ::GALL-CLB2::URA3 clb3Δ::TRP1 clb4Δ::his3::kanMX clb5Δ::kanMX clb6Δ::kanMX swe1Δ::TRP1 PGK1pr::PGK1pr-EL222, LIP-CLB2kd::NatMX ADE2*	This study
yVG604	*cdh1Δ::LEU2 cdc20Δ::MET3pr-CDC20::TRP1 CLN2pr-GFP-CLN2pest::HIS3 PGK1pr::PGK1pr-EL222, LIP-CDC20::NatMX*	This study
yVG152	*cln1Δ cln2Δ::CLN2pr-Venus::TRP1 cln3Δ::LEU2 trp1Δ::MET3-CLN2::TRP1 clb3Δ::TRP1 clb4Δ::his3::KanMX clb6Δ::KanMX HTB2::HTB2-mCherry::HIS5 PGK1pr::PGK1pr-EL222, LIP-CLB5::NatMX*	This study
yVG2371	*cln1Δ cln2Δ cln3Δ::LEU2 trp1Δ::MET3pr::CLN2 ycr051wΔ::PGL1pr-EL222, LIP-CLN2::NatMX*	This study
yVG2374	*cln1Δ cln2Δ cln3Δ::LEU2 trp1Δ::MET3pr::CLN2 ycr051wΔ::PGL1pr-EL222, LIP-CLB5::NatMX*	This study
yVG2390	*cln1Δ cln2Δ cln3Δ::LEU2 clb3Δ::TRP1 clb4Δ::his3::KanMX clb5Δ::HIS3 clb6Δ::KanMX HTB2::HTB2-mCherry::HIS5 POL3::POL3 (Leu523Asp)::hphMX EFB1pr::PGK1pr-EL222, LIP-CLB5::NatMX* *pRD-TW1 (CEN/ARS)*	This study
yVG1247	*cln1Δ cln2Δ cln3Δ::LEU2 clb3Δ::TRP1 clb4Δ::his3::KanMX clb5Δ::HIS3 clb6Δ::KanMX HTB2::HTB2-mCherry::HIS5 POL3::POL3 (Leu523Asp)::hphMX EFB1pr::PGK1pr-EL222, LIP-CLN2, LIP-CLB5::NatMX* (single copy)	This study
yVG1358	*cln1Δ cln2Δ cln3Δ::LEU2 clb3Δ::TRP1 clb4Δ::his3Δ::KanMX clb5Δ::HIS3 clb6Δ::KanMX HTB2::HTB2-mCherry::HIS5 POL3::POL3 (Leu523Asp)::hphMX sic1Δ::URA3 EFB1pr::PGK1pr-EL222, LIP-CLN2, LIP-CLB5::NatMX* (single copy)	This study
yVG1623	*ura3Δ::LIP-yEVenus::KanMX* (single copy)	Ref. [88]
yVG2840	*ycr051wΔ::LIP-ymScarletI::URA3* (single copy)	This study
yVG2842	*his3Δ::PGK1pr-EL222::HIS3* (single copy)	This study

	ycr051wΔ::LIP-ymScarletI-PEST::URA3 (single copy)	
yVG1637	*his3Δ::PGK1pr-EL222::HIS3* (single copy) *ura3Δ::LIP-yEVenus::KanMX* (single copy)	Ref. [88]
yVG2844	*his3Δ::PGK1pr-EL222 (Asp18Tyr, Val139Leu)::HIS3* (single copy) *ura3Δ::LIP-yEVenus::KanMX* (single copy)	This study
yVG2846	*his3Δ::PGK1pr-EL222 (Asp18Tyr)::HIS3* (single copy) *ura3Δ::LIP-yEVenus::KanMX* (single copy)	This study
yVG2848	*his3Δ::PGK1pr-EL222 (Val139Leu)::HIS3* (single copy) *ura3Δ::LIP-yEVenus::KanMX* (single copy)	This study
yVG2850	*his3Δ::PGK1pr-EL222 (Lys99Glu)::HIS3* (single copy) *ura3Δ::LIP-yEVenus::KanMX* (single copy)	This study
yVG2852	*his3Δ::PGK1pr-EL222 (Pro165Ser)::HIS3* (single copy) *ura3Δ::LIP-yEVenus::KanMX* (single copy)	This study
yVG2854	*his3Δ::PGK1pr-EL222 (Val201Leu)::HIS3* (single copy) *ura3Δ::LIP-yEVenus::KanMX* (single copy)	This study
yVG2701	*his3Δ::PGK1pr-EL222 (Asp89Tyr)::HIS3* (single copy) *ycr051wΔ::LIP-ymScarletI::URA3* (single copy)	This study
yVG2750	*his3Δ::PGK1pr-EL222 (Gly94Cys)::HIS3* (single copy) *ycr051wΔ::LIP-ymScarletI::URA3* (single copy)	This study
yVG2704	*his3Δ::PGK1pr-strongLOV::HIS3* (single copy) *ycr051wΔ::LIP-ymScarletI::URA3* (single copy)	This study
yVG2726	*his3Δ::PGK1pr-EL222 (Leu87Ile)::HIS3* (single copy) *ycr051wΔ::LIP-ymScarletI::URA3* (single copy)	This study
yVG1645	*his3Δ::PGK1pr-EL222 (Ala157Val)::HIS3* (single copy) *ura3Δ::LIP-yEVenus::KanMX* (single copy)	This study
yVG2759	*his3Δ::PGK1pr-EL222 (Gly80Glu)::HIS3* (single copy) *ycr051wΔ::LIP-ymScarletI::URA3* (single copy)	This study
yVG2703	*his3Δ::PGK1pr-EL222 (Gly82Val)::HIS3* (single copy) *ycr051wΔ::LIP-ymScarletI::URA3* (single copy)	This study
yVG2706	*his3Δ::PGK1pr-EL222 (Thr83Ser)::HIS3* (single copy) *ycr051wΔ::LIP-ymScarletI::URA3* (single copy)	This study
yVG2761	*his3Δ::PGK1pr-AQTrip (yeast codon optimized)::HIS3* (single copy)	This study

	ycr051wΔ::LIP-ymScarletI::URA3 (single copy)	
yVG2752	*his3Δ::PGK1pr-EL222 (Ser137Asn)::HIS3* (single copy) *ycr051wΔ::LIP-ymScarletI::URA3* (single copy)	This study
yVG2727	*his3Δ::PGK1pr-EL222 (Val121Met)::HIS3* (single copy) *ycr051wΔ::LIP-ymScarletI::URA3* (single copy)	This study
yVG2753	*his3Δ::PGK1pr-EL222 (Glu84Lys)::HIS3* (single copy) *ycr051wΔ::LIP-ymScarletI::URA3* (single copy)	This study
yVG2699	*his3Δ::PGK1pr-EL222 (Thr83Ala)::HIS3* (single copy) *ycr051wΔ::LIP-ymScarletI::URA3* (single copy)	This study
yVG2714	*his3Δ::PGK1pr-EL222 (Glu104Gly)::HIS3* (single copy) *ycr051wΔ::LIP-ymScarletI::URA3* (single copy)	This study
yVG2725	*his3Δ::PGK1pr-EL222 (Cys75Arg)::HIS3 (single copy)* *ycr051wΔ::LIP-ymScarletI::URA3* (single copy)	This study
yVG2715	*his3Δ::PGK1pr-EL222 (Thr88Pro)::HIS3* (single copy) *ycr051wΔ::LIP-ymScarletI::URA3* (single copy)	This study
yVG2721	*his3Δ::PGK1pr-EL222 (Gly136Ser)::HIS3 (single copy)* *ycr051wΔ::LIP-ymScarletI::URA3* (single copy)	This study
yVG2709	*his3Δ::PGK1pr-EL222 (Val103Phe)::HIS3* (single copy) *ycr051wΔ::LIP-ymScarletI::URA3* (single copy)	This study
yVG1031	*ura3Δ::GAL1pr-yEVenus::KanMX*	Ref. [88]
yVG301	*ura3Δ::GAL1pr-yEVenus-PEST::URA3*	Ref. [88]
yVG151	*PHYB-mCherry-Tom7::LEU2; Bem1-mCitrine-PIF::HIS3*	Ref. [150]
yVG2839	*PHYB-mCherry-Tom7::LEU2; Bem1-mCitrine-PIF::HIS3 yor1::hphMX*	This study
yVG2837	*leu2Δ::ADH1pr-GADPIF3::LEU2, trp1::ADH1pr-PHYB-GDBD::TRP1, his3Δ::GAL1pr-YFP::HIS3, ade2::ADE2*	Ref. [110]
yVG2838	*leu2Δ::ADH1pr-GADPIF3::LEU2, trp1::ADH1pr-PHYB-GDBD::TRP1, his3Δ::GAL1pr-YFP::HIS3, ade2::ADE2 yor1::hphMX*	This study
yVG2691	*cln1Δ cln2Δ cln3Δ::LEU2 clb3::TRP1 clb4Δ::his3Δ::KanMX clb5Δ::HIS3 clb6Δ::KanMX HTB2::HTB2-mCherry::HIS5 ycr051wΔ::PGK1pr-EL222, LIP-PEST-rtTA, tetOpr-CLN2::NatMX*	This study

	BUD23::tetOpr-CLB5::PatMX	
yVG2856	*his3Δ::PGK1pr-PEST-rtTA::HIS3* (single copy) *ura3Δ::tetOpr-yEVenus-PEST::URA3* (single copy)	This study
yVG2857	*his3Δ::PGK1pr-PEST-rtTA (Phe67Cys)::HIS3* (single copy) *ura3Δ::tetOpr-yEVenus-PEST::URA3* (single copy)	This study
yVG2858	*his3Δ::PGK1pr-PEST-rtTA (Arg253Hys)::HIS3* (single copy) *ura3Δ::tetOpr-yEVenus-PEST::URA3* (single copy)	This study

1526

1527

1528 Supplementary Table 3. Number of cells analyzed in Figure 2 B

Experiment	Number of scored cells
LIP-CLB5 cln1-3Δ 20 min pulse	53
LIP-CLB5 cln1-3Δ 40 min pulse	30
LIP-CLN2 cln1-3Δ 20 min pulse	27
LIP-CLN2 cln1-3Δ 40 min pulse	20
LIP-CLB5 cln1-3Δ clb3-6Δ pRD-TW1 20 min	129
LIP-CLB5 LIP-CLN2 cln1-3Δ clb3-6Δ pRD-TW1 40 min	42

1529

1530

1531 Supplementary Table 4. Distribution of mutation types across campaigns 1-3 for *EL222* compared
1532 to the WT budding yeast mutation spectrum from ref.[194]

Mutation	Count	Percentage	WT budding yeast mutation spectrum[194]
T>C	6	22%	14%
T>A	2	7%	6%
T>G	3	11%	11%
C>A	8	30%	18%
C>G	0	0%	15%
C>T	8	30%	35%
Total transitions	14	52%	49%
Total transversions	13	48%	51%

1533

1534

1535

1536

1537 Supplementary Table 5. Number of cells analyzed in Figure 4 B

	WT EL222	G94C	V121M	A157V	S137N	G80E	D89Y	AQTrip	T83S	E84K	strongLOV	G82V	L87I
Darkness	246	234	424	144	206	341	341	275	126	227	478	239	248
Low blue LED	329	48	344	155	76	117	151	58	107	81	84	93	93
High blue LED	374	60	320	283	67	58	88	83	95	274	100	43	57

1538

1539

1540

1541 Supplementary Table 6. Number of cells analyzed in Figure 4 C, G, and K

Figure	mutant	N at 3.5 h
4 C	*wt-EL222*	267
4 C	T83S	105
4 C	G82V	77
4 C	L87I	119
4 C	G80R	79
4 C	A157V	92
4 G	*wt-EL222*	93
4 G	K99E	68
4 G	V201L	31
4 K	*wt-EL222*	121
4 K	T83A	40

1542

1543

1544 Supplementary Table 7. Number of cells analyzed in Figure 4 F

	V201L	D31Y, V139L	K99E	P165S	D31Y	V139L	WT EL222
Darkness	112	479	188	238	208	362	246
Low blue LED	325	203	330	81	419	209	329
High blue LED	209	382	321	98	466	441	374

1545

1546

1547

1548 Supplementary Table 8. Number of cells analyzed in Figure 4 J

	WT EL222	E104G	T83A	C75R	V103F	T88P	G136S	E84K	L87P	V41F	E84G
Darkness	246	142	65	135	262	80	141	227	386	149	175
High blue LED	374	107	539	158	558	486	70	274	328	220	96
λ = 488 nm	438	119	219	326	160	241	303	615	270	193	685
λ = 514 nm	244	166	256	313	230	261	187	264	420	126	180
λ = 561 nm	177	267	175	141	204	182	188	204	197	156	101
λ = 651 nm	202	237	113	232	191	189	183	269	275	278	206

1549

1550

1551

1552 Supplementary Table 9. Number of cells analyzed in Figure 5 C

	Darkness, no PCB	Darkness, PCB	Light, no PCB	Light, PCB
yor1Δ	133	75	143	71
YOR1	186	83	181	190

1553

1554

1555

1556 Supplementary Table 10. Number of cells analyzed in Figure 6 D

	WT	F67C	R253H
+ Dox	220	506	467
- Dox	178	273	321

1557

1558

1559

1560 Supplementary Table 11. Number of cells analyzed in Supplementary Figure 2.

	AX42	LIP-yEVenus	WT EL222
Darkness	229	433	246

1561

1562

1563

1564 Supplementary Table 12. Number of cells analyzed in Supplementary Figure 3.

	D89Y	V103I	P114L	Y108H	P114R	WT EL222	strongLOV	I105V	G80R	T83A	V121L	E104G	T88P	C75R	V103F	L87P	E84K	G136S	V41F	E84G
Darkness	341	183	110	133	217	246	478	114	240	65	198	142	80	135	262	386	227	141	149	175
514 nm	198	331	230	272	324	244	502	105	365	256	127	166	261	313	230	420	264	187	126	180

1565

1566